RSC Advances

PAPER

View Article Online
View Journal | View Issue

Cite this: *RSC Adv.*, 2024, **14**, 34643

Novel carboranyl-BODIPY conjugates: design, synthesis and anti-cancer activity†

Chandra Sekhara Mahanta,[a] Sunitee Hansdah,[b] Kabita Khuntia,[b] Bibhuti Bhusan Jena,[a] Biswa Ranjan Swain,[a] Subhadeep Acharya,[a] Barada Prasanna Dash,*[c] Priya Ranjan Debata*[b] and Rashmirekha Satapathy*[a]

A series of four carboranyl-BODIPY conjugates (***o*-CB-10**, ***m*-CB-15**, **Me-*o*-CB-28**, and **Me-*o*-CB-35**) and one phenylene-BODIPY conjugate (**PB-20**) were synthesized. The carboranyl-BODIPY conjugates incorporate boron clusters, specifically *ortho*- and *meta*-carboranes, covalently linked to BODIPY fluorophores while the phenylene-BODIPY conjugate features a phenylene ring covalently linked to BODIPY fluorophore. The newly synthesized conjugates were characterized by ^{1}H NMR, ^{13}C NMR, ^{11}B NMR, ^{19}F NMR, FT-IR, and high-resolution mass spectral analysis. *In vitro* cytotoxicity of the synthesized conjugates has been evaluated against the HeLa cervical cancer cell line. The study reveals that ***o*-CB-10** shows a maximum cell death potential at lower concentrations (12.03 μM) and inhibited cell proliferation and migration in cancer (HeLa) cells. Additionally, flow cytometry study reveals that ***o*-CB-10** and **Me-*o*-CB-28** arrest the cell cycle at the S phase. The results indicate that the carboranyl-BODIPY conjugates have the potential to be effective anticancer agents.

Received 8th October 2024
Accepted 23rd October 2024

DOI: 10.1039/d4ra07241c

rsc.li/rsc-advances

1. Introduction

Icosahedral carboranes are often regarded as three-dimensional analogues of benzene.[1] They exist in three isomers such as *ortho*-, *meta*- and *para*-carborane distinguished by the relative positions of the two carbon atoms within the icosahedral cage (Fig. 1). They display distinctive electronic and molecular structures,[2] which have been applied to a variety of applications such as in medicinal chemistry,[3–12] material science[13–29] and organometallic/coordination chemistry.[30–36] Derivatives of icosahedral carboranes showed cytotoxicity towards several cancer cells. Continuous efforts have been devoted by researchers to conjugate carboranes with several tumour targeting moieties such as amino acids,[37–39] receptor-specific membrane antigens,[40–43] porphyrins,[44–46] micelles,[47–49] polymeric nanoparticles,[50–53] peptides,[54] liposomes,[55] dendrimers,[56,57] carbohydrates,[58–60] and BODIPY,[61,62] *etc.* to enhance the therapeutic effect of the drugs for selective and effective treatment of cancer in addition to their application in boron neutron capture therapy (BNCT). Two boron-based drugs, sodium mercaptododecaborate (BSH) and boronophenylalanine (BPA), have clinically demonstrated efficacy as BNCT agents[63] (Fig. 1). Moreover, derivatives of icosahedral carboranes have also shown cytotoxicity towards glioma cells.[64,65]

4,4-Difluoro-4-bora-3*a*,4*a*-diaza-*s*-indacene, commonly referred to as BODIPY, is a compound in which BF_2 is chelated to dipyrromethene, the half form of porphyrin. BODIPY-based compounds have garnered significant interest due to their versatility across various applications, including drug administration,[66–69] bioimaging,[70–79] photodynamic treatment[80–82] (PDT), and artificial photosynthetic systems.[83–85] Notably, these compounds exhibit a preferential accumulation in tumor tissue, creating favorable tumor-to-healthy tissue ratios, thereby rendering them promising candidates for boron neutron capture therapy (BNCT).[86] Moreover, BODIPY can be easily modified to include biological capabilities without affecting its inherent features.

Despite significant progress in therapy, cancer continues to be a prominent cause of death worldwide. Existing therapeutic methods, such as chemotherapy, frequently have limited effectiveness because of the occurrence of unwanted side effects and the emergence of drug resistance.[87] These issues arise from the inability to specifically target cancer cells while maintaining the integrity of healthy tissues. Tumorigenesis is a dynamic process characterized by genetic, epigenetic, and metabolic changes that disturb the normal cell cycle.[88,89] Cancer cells avoid programmed cell death (apoptosis) and alter cell cycle checkpoints, resulting in uncontrolled replication.[90] In the cell cycle,

[a]*Department of Chemistry Ravenshaw University College Square, Cuttack 753003, Odisha, India. E-mail: rashmi.satapathy@gmail.com*

[b]*Department of Zoology Maharaja Sriram Chandra Bhanja Deo University, Sri Ram Chandra Vihar, Takatpur, Mayurbhanj, Baripada 757003, Odisha, India. E-mail: prdebata@gmail.com*

[c]*Department of Chemistry, Rajdhani College, Bhubaneshwar 751003, India. E-mail: barada.dash@gmail.com*

† Electronic supplementary information (ESI) available: The exact experimental procedures and full characteristics. See DOI: https://doi.org/10.1039/d4ra07241c

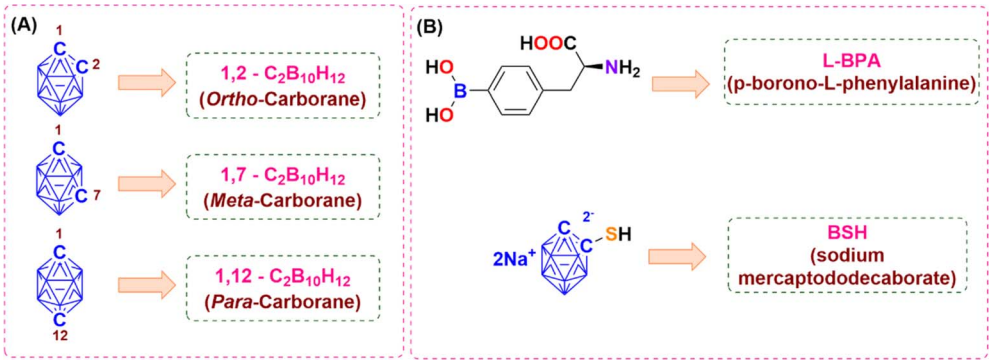

Fig. 1 (A) Three isomers of icosahedral carborane. (B) Clinically approved boron-based drugs as anti-cancer agents.

a sequence of events leading to cell division is typically controlled by checkpoints during the G1/S, S, and G2/M phases. Cancer cells evade these regulatory checkpoints, allowing uncontrolled proliferation. Targeting proteins involved in the course of the cell cycle has become a viable technique for treating cancer.[91]

Multiple chemicals have been formulated to disrupt the course of the cell cycle. Flavopiridol, for example, hinders cyclin-dependent kinases (CDKs), resulting in the halting of the cell cycle in both the G1 and G2 stages.[92] Indisulam (E7070), a compound derived from sulfonamide derivative, causes cells to stop in the G1 phase of the cell cycle and slows down the transition from G1 to the S phase, and finally results in cells being arrested in the G2 phase and undergoing apoptosis.[93] Additional drugs, including AZD5438, SNS-032, bryostatin-1, seliciclib, PD 0332991, and SCH 727965, demonstrate inhibitory effects on the cell cycle at various phases.[94]

So, developing novel chemotherapeutic medications that can specifically target and eliminate cancer cells while limiting harm to healthy organs is crucial. In 2020, our research group developed triazine-cored dendritic molecules containing multiple *o*-carborane clusters and investigated their cytotoxicity against breast cancer cell lines.[4] In the same year, we reported the synthesis of a series of carborane-appended glycoconjugates with selective cytotoxicity towards MCF-7 breast cancer cells and A431 skin cancer cells over healthy cells.[6] Additionally, we also developed star-shaped phenylene BODIPY and conducted toxicity and biocompatibility evaluations on zebrafish.[66] In 2023, dendritic glycoconjugates containing multiple *o*-carborane clusters were synthesized, and their anti-cancer efficacy was studied against MCF-7 breast cancer cell lines.[56] These findings inspired us to continue the bioactivity exploration of carborane and BODIPY-based molecules. Herein, we report the synthesis of four carboranyl-BODIPY conjugates: *ortho*-carboranyl BODIPY 10 (***o*-CB-10**), *meta*-carboranyl BODIPY 15 (***m*-CB-15**), methylene bridged *ortho*-carboranyl BODIPY 28 (**Me-*o*-CB-28**) and methylene bridged *ortho*-carboranyl BODIPY 35 containing two carborane moieties (**Me-*o*-CB-35**) along with one phenylene-BODIPY conjugate 20 (**PB-20**). Biological evaluation of these compounds was carried out against HeLa cervical cancer cell lines to explore the ability of the synthesized carboranyl BODIPYs as anti-cancer therapeutics.

2. Results and discussion

2.1 Synthesis

Four carboranyl-BODIPY conjugates (***o*-CB-10**, ***m*-CB-15**, **Me-*o*-CB-28**, and **Me-*o*-CB-35**) and one phenylene-BODIPY conjugate (**PB-20**) were designed and successfully synthesized following several reaction conditions. Synthetic methods like Sonogashira cross-coupling reaction, Suzuki cross-coupling reaction, decaborane insertion, PCC mediated oxidation, base promoted substitution reaction, *etc.* were involved in addition to TFA catalyzed preparation of dipyrromethane, DDQ mediated formation of dipyrromethene and subsequent BF_3. OEt_2 promoted the formation of BODIPY in the presence of a base like Et_3N. All the newly synthesized compounds were well characterized through FT-IR, NMR, and mass spectral analysis (see ESI†).

2.1.1 Synthesis of *ortho*-carboranyl BODIPY 10 (*o*-CB-10). Synthesis of *ortho*-carboranyl BODIPY **10** (***o*-CB-10**) was carried out starting from commercially available compound 1-bromo-4-iodobenzene **1** as shown in Scheme 1. The reaction of compound **1** with trimethylsilyl acetylene **2** under Sonogashira cross-coupling reaction conditions afforded compound **3** with excellent yield. K_2CO_3 promoted deprotection of the TMS group in compound **3**, which yielded alkynylated compound **4** in good yield. *Ortho*-carborane appended derivative **5** was synthesized upon decaborane insertion reaction of compound **4** in acetonitrile. Subsequently, the *ortho*-carborane appended aldehyde **7** was formed *via* Suzuki coupling reaction in the presence of mild base Cs_2CO_3. The condensation of compound **7** with compound **8** in the presence of trifluoroacetic acid (TFA) produced *o*-carboranyl dipyrromethane **9**. The resultant *o*-carboranyl dipyrromethane subsequently oxidized using 2,3-dichloro-5,6-dicyano-*p*-benzoquinone (DDQ) to afford the stable *ortho*-carborane appended dipyrromethene which undergone deprotonation in basic conditions using Et_3N before being exposed to excess $BF_3 \cdot OEt_2$and formed the desired ***o*-CB-10** with 41% yield. Substituted pyrrole **8** used in the synthesis of dipyrromethene derivatives was prepared in three steps in accordance with the reported procedure.[95]

2.1.2 Synthesis of *meta*-carboranyl BODIPY 15 (*m*-CB-15). Starting from BuLi mediated reaction of *meta*-carborane **11**, ***m***-

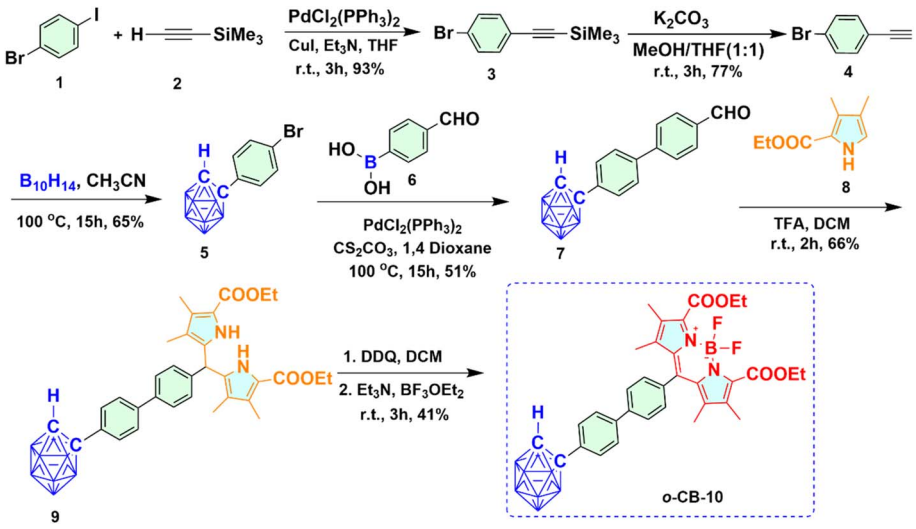

Scheme 1 Synthetic route for *ortho*-carboranyl BODIPY **10** (*o*-**CB-10**).

CB-15 was prepared as depicted in Scheme 2. At first, the C-arylated mono-bromo derivative of *m*-carborane **12** was synthesized from the reaction of *meta*-carborane **11** with compound **1** *via* reported Cu(I) mediated approach in the presence of strong base like BuLi followed by purification using column chromatography and sublimation. Upon reaction of compound **12** with 4-formyl phenyl boronic acid **6** under Suzuki cross-coupling reaction conditions, *meta*-carboranyl C-aryl aldehyde **13** was prepared in good yield. Trifluoroacetic acid (TFA) catalyzed condensation of compound **13** with compound **8** produced *meta*-carboranyl dipyrromethane **14** in decent yield as a white solid. The resultant *m*-carboranyl dipyrromethane **14** subsequently oxidized to *m*-carboranyl dipyrromethene derivative using DDQ, and upon addition of Et_3N followed by $BF_3 \cdot OEt_2$ to the same reaction mixture, ***m*-CB-15** was synthesized as red solid with 38% yield.

2.1.3 Synthesis of phenylene BODIPY 20 (PB-20). To find out the effect of *o*- and *meta*-carborane on the properties of BODIPY derivatives, **PB-20** was synthesized by starting from the Suzuki coupling reaction of compound **1** with phenylboronic acid **16** as presented in Scheme 3. The reaction of compound **1** with compound **16** catalysed by $PdCl_2(PPh_3)_2$ in presence of Na_2CO_3 afforded compound **17** in 81% yield. Again, under the Suzuki coupling condition, the corresponding aldehyde **18** was prepared upon reaction of compound **17** with 4-formylphenyl boronic acid **6** with 65% yield. Phenylene dipyrromethane **19** was synthesized with 64% yield upon treatment of compound **18** with substituted pyrrole **8** catalyzed by trifluoroacetic acid (TFA). Finally, in one pot reaction, oxidation of dipyrromethane **19** was carried out using DDQ to form phenylene dipyrromethene derivative, which upon treatment with Et_3N and $BF_3 \cdot OEt_2$ afforded **PB-20** as red solid in 42% yield.

2.1.4 Synthesis of methylene bridged *ortho*-carboranyl BODIPY 28 (Me-*o*-CB-28). Synthetic routes used to obtain **Me-*o*-CB-28** is shown in Scheme 4. Synthesis of BODIPY **28** containing one *ortho*-carborane moiety was achieved starting from a base-promoted nucleophilic substitution reaction. Commercially available methyl-4-hydroxybenzoate **21** and propargyl bromide

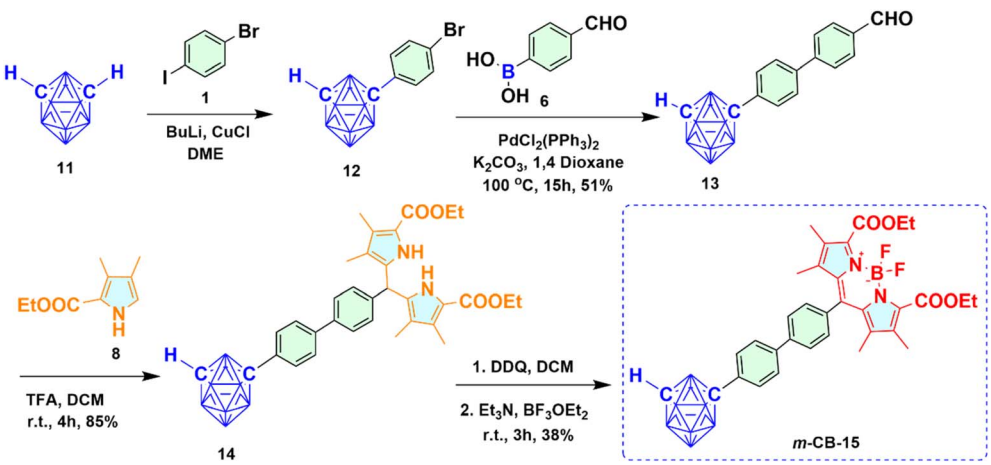

Scheme 2 Synthetic route for *meta*-carboranyl BODIPY **15** (*m*-**CB-15**).

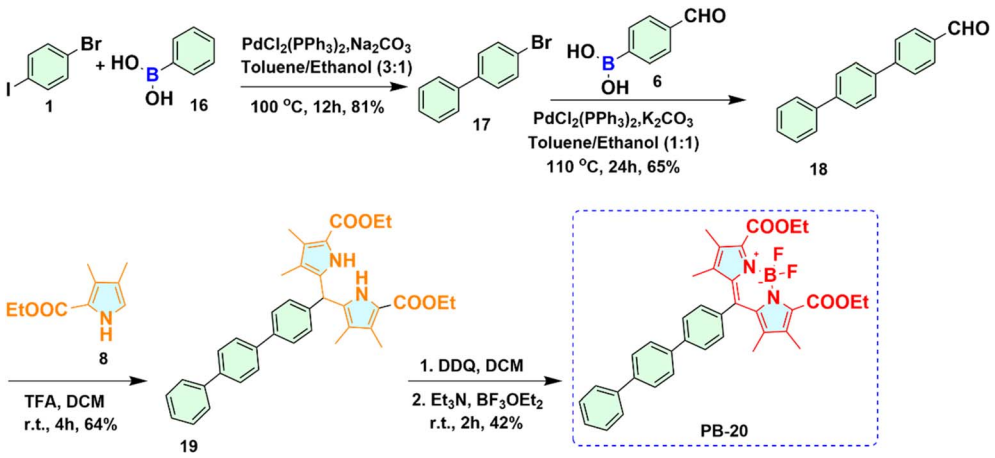

Scheme 3 Synthetic route for phenylene BODIPY **20** (**PB-20**).

22 underwent a nucleophilic substitution reaction in the presence of base K_2CO_3 to get alkyne derivative **23** with 86% yield. 4-(Prop-2-ynyloxy) phenyl methanol **24** was obtained upon reduction of the ester group of compound **23** with $LiAlH_4$. The primary alcohol group of compound **23** oxidized to 4-(Prop-2-ynyloxy) benzaldehyde **25** using pyridinium chlorochromate (PCC) as an oxidizing agent. To prevent the reduction of the aldehyde group to primary alcohol in the presence of decaborane, compound **25** was first converted to dipyrromethane **26**, and then the *o*-carborane cage was formed upon refluxing with decaborane. Trifluoroacetic acid (TFA) catalyzed the reaction of compound **25** with substituted pyrrole **8** in dichloromethane, afforded dipyrromethane **26** with 66% yield. *Ortho*-carboranyl dipyrromethane conjugate **27** was prepared from compound **26** upon refluxing with decaborane. In a one-pot reaction system, the resultant *o*-carboranyl dipyrromethane **27** underwent an oxidation reaction using 2,3-dichloro-5,6-dicyano-*p*-benzoquinone (DDQ), yielding *o*-carboranyl dipyrromethene monitored by TLC. To the same reaction mixture, subsequent addition of triethyl amine followed by $BF_3 \cdot OEt_2$ provided the desired **Me-*o*-CB-28** in 39% yield as a red solid.

2.1.5 Synthesis of methylene bridged *ortho*-carboranyl BODIPY 35 containing two carborane moieties (Me-*o*-CB-35). Under a similar approach as described in the preparation of **Me-*o*-CB-28**, carboranyl BODIPY **35** containing two *ortho*-carborane cages was prepared as deep red solid shown in Scheme 5. The reaction of commercially available methyl-3,5-dihydroxybenzoate **29** with propargyl bromide **22** in the presence of base K_2CO_3 yielded alkyne derivative **30**, which upon subsequent reduction with $LiAlH_4$ provided compound **31** with a decent yield. PCC-mediated oxidation of compound **31** afforded formyl compound **32** with 85% yield. Trifluoroacetic acid (TFA) catalyzed the reaction of compound **32** with substituted pyrrole **8**, afforded dipyrromethane **33** with 66% yield, which,

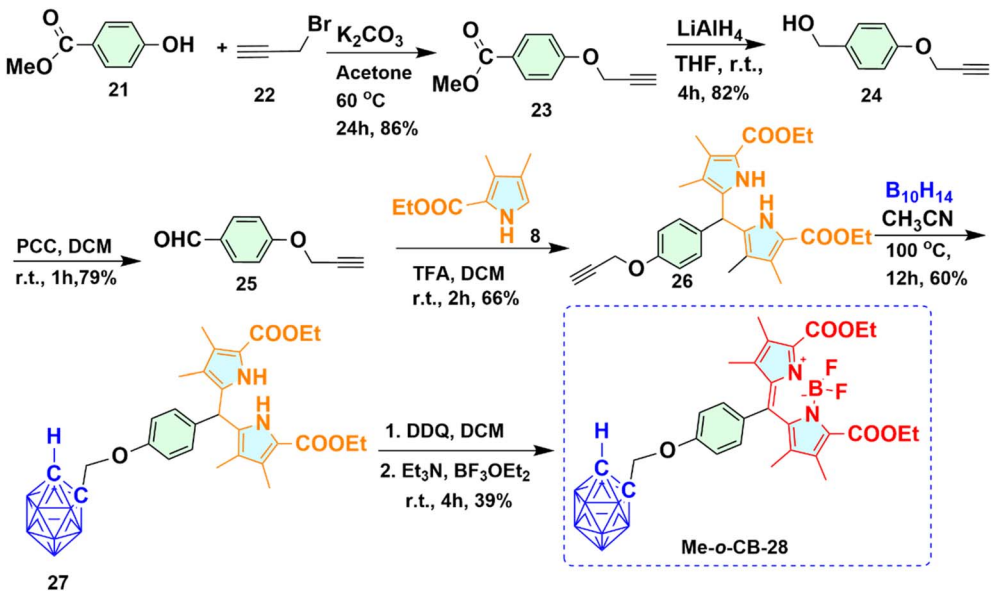

Scheme 4 Synthetic route for methylene bridged *ortho*-carboranyl BODIPY **28** (**Me-*o*-CB-28**).

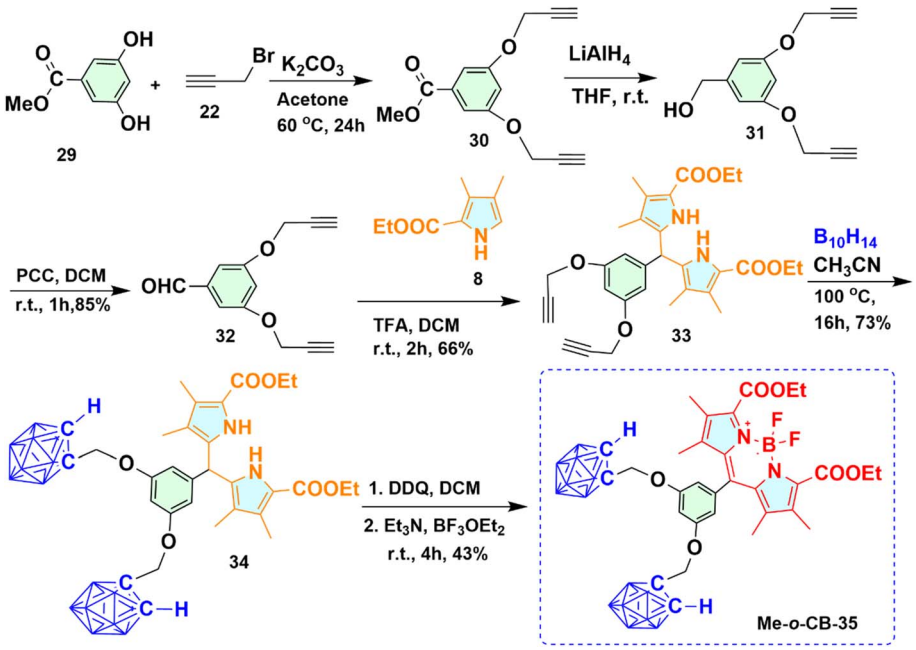

Scheme 5 Synthetic route for methylene bridged carboranyl BODIPY **35** (**Me-*o*-CB-35**) having two *ortho*-carborane moieties.

upon refluxed with decaborane compound **34** containing two carborane moieties, was prepared. The resultant *ortho*-carboranyl dipyrromethane **34** underwent oxidation with DDQ forming *o*-carboranyl dipyrromethene checked by TLC. Subsequent addition of triethyl amine and $BF_3 \cdot OEt_2$ provided the desired **Me-*o*-CB-35** in 43% yield.

The final BODIPY conjugates ***o*-CB-10**, ***m*-CB-15**, **Me-*o*-CB-28**, **Me-*o*-CB-35**, and **PB-20** were confirmed from ^{1}H NMR, ^{13}C NMR, ^{11}B NMR, ^{19}F NMR, FT-IR and high-resolution mass spectral evidence. All conjugates exhibited solubility in DMSO solvent. In all BODIPY compounds, the disappearance of the –NH proton peak around $\delta = 8.43$–9.26 ppm and *meso* proton around

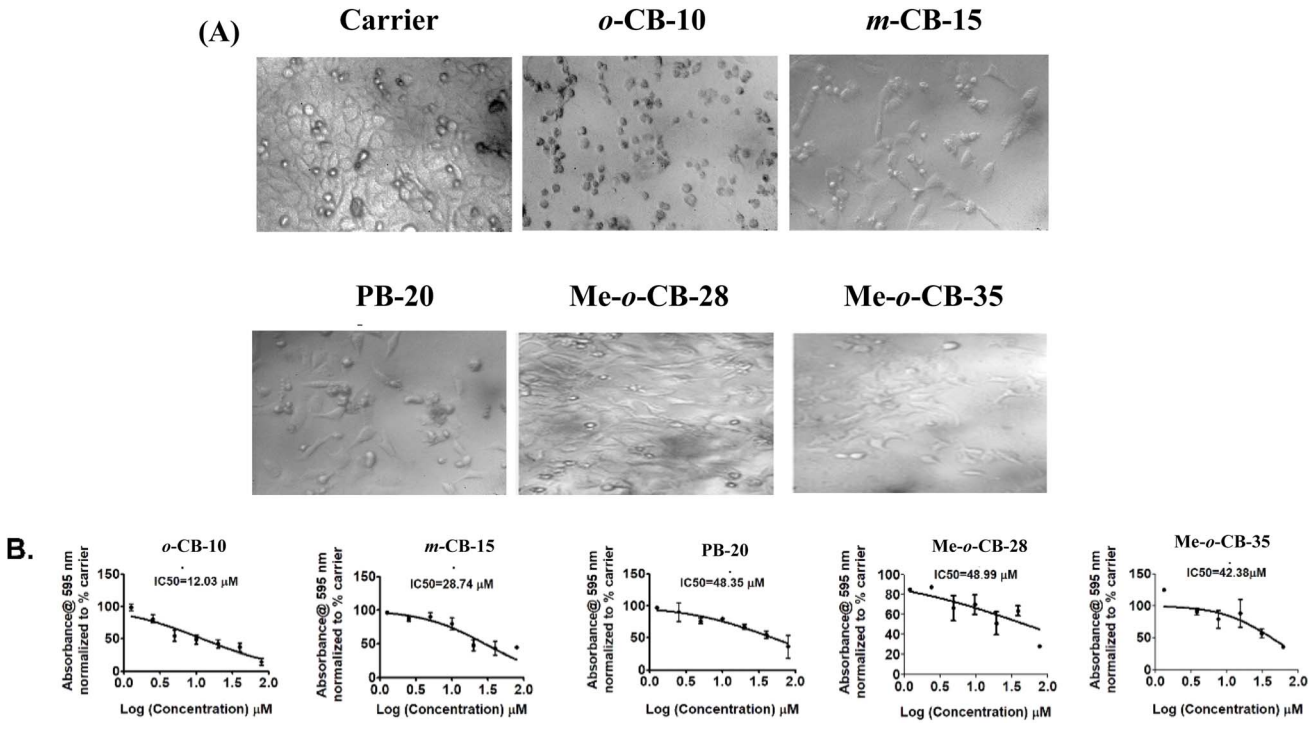

Fig. 2 (A) Representative images of the HeLa cells treated with carrier (DMSO) or 10 μM concentrations of each of the compounds ***o*-CB-10**, ***m*-CB-15**, **PB-20**, **Me-*o*-CB-28** and **Me-*o*-CB-35** for 72 h on HeLa cells. The compound ***o*-CB-10** shows highest degree of cell death in comparison to others (B) Represents the dose inhibitory curve determined by MTT cell viability assay. The IC_{50} values are indicated in the graph. Results are expressed as the mean ± standard error.

$\delta = 5.5$ ppm in ^{1}H NMR spectra indicated the formation of BODIPY conjugates. The presence of the BF_2 group in BODIPY conjugates was evident from ^{11}B NMR and ^{19}F NMR spectral data. The presence of fluorine was confirmed from ^{19}F NMR spectral analysis, which showed a 1 : 1 : 1 : 1 quartet in the range $\delta = -140$ to $\delta = -141$ ppm. In proton decoupled ^{11}B NMR spectra of BODIPY conjugates, a triplet peak is observed in the range $\delta = -0.23$ to $\delta = -0.85$, corresponding to BF_2 boron. In ^{13}C NMR spectra appearance of peaks around $\delta = 60$ ppm and $\delta = 75$ ppm for two cage carbons and in proton decoupled ^{11}B NMR spectra resonance of peaks in the range $\delta = 0$ ppm to $\delta = -15$ ppm confirms the presence of carborane cage/s in carboranyl BODIPY conjugates. FT-IR spectral analysis showed strong bands around $\nu_{str} = 2600$ cm^{-1} corresponding to B–H stretching in all carboranyl BODIPY conjugates. The anti-cancer efficacy of the synthesized BODIPYs against HeLa cervical cancer cells were investigated through *in vitro* cytotoxicity, cell proliferation activity, cell migration activity, and p53 expression study. Flow cytometry study was also carried out to explore at which phase the synthesized BODIPYs able to inhibit the HeLa cell cycle progression.

2.2 Biological evaluation

2.2.1 Cytotoxicity of BODIPY conjugates (*o*-CB-10, *m*-CB-15, Me-*o*-CB-28, Me-*o*-CB-35, and PB-20) on HeLa cell viability. The anti-cancer efficacy of the BODIPY conjugates (***o*-CB-10**, ***m*-CB-15**, **Me-*o*-CB-28**, **Me-*o*-CB-35**, and **PB-20**) against Human Cervical cancer cells (HeLa cells) were investigated. Fig. 2A illustrates the results of *in vitro* cytotoxicity studies conducted with BODIPY conjugates against HeLa cells after 72 hours, and dose-dependent cytotoxic effects were observed. The half-

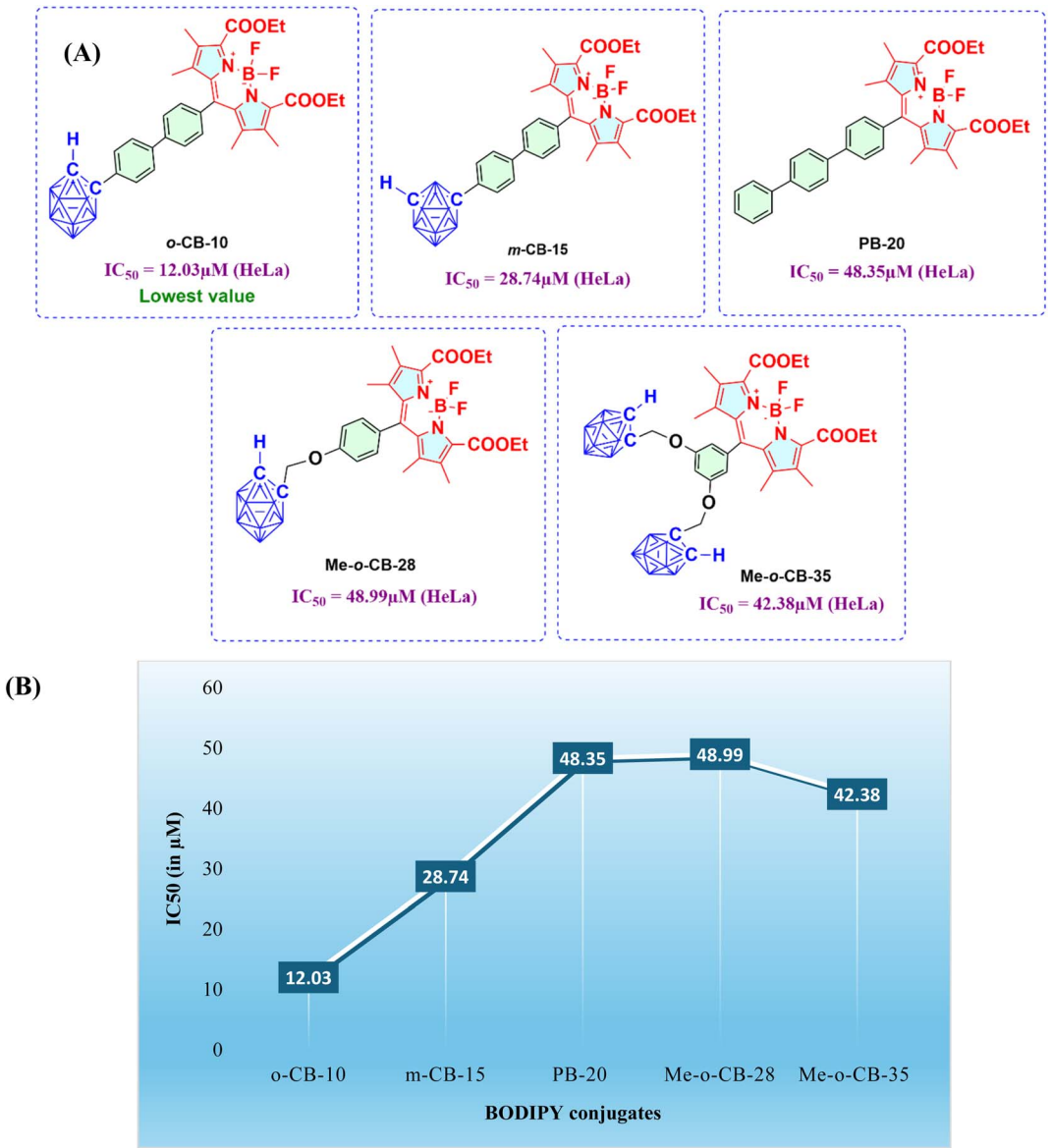

Fig. 3 (A) Shows the IC_{50} values of compounds ***o*-CB-10**, ***m*-CB-15**, **PB-20**, **Me-*o*-CB-28**, **Me-*o*-CB-35**. (B) Table showing trends in IC_{50} values BODIPY-conjugates.

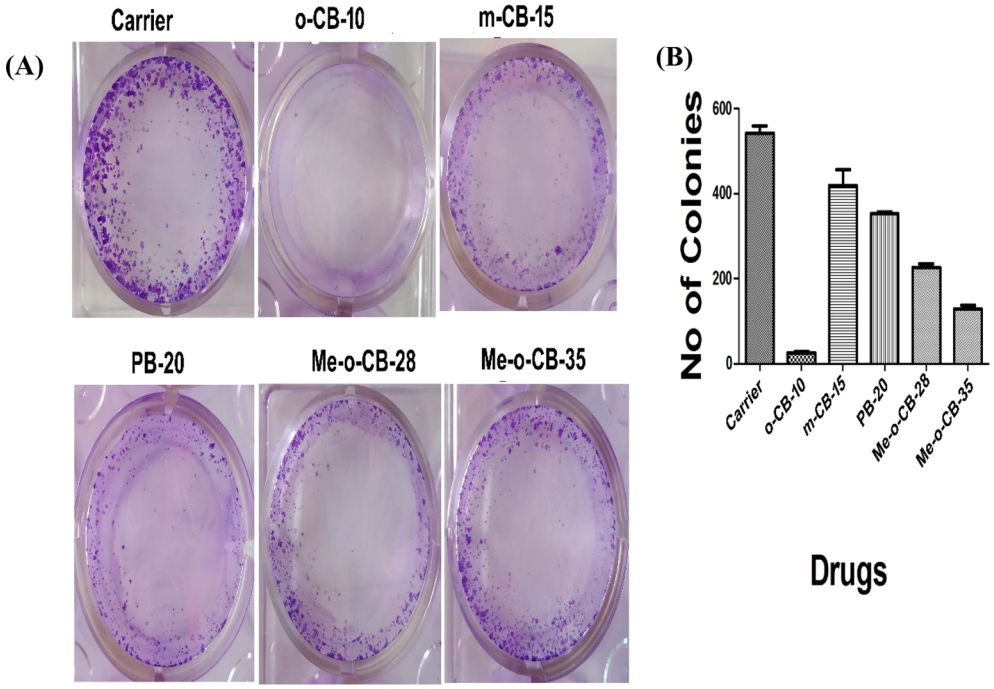

Fig. 4 (A) Colony forming assay of HeLa cells. Cells were treated with carrier or 10 μM each of BODIPY conjugates in 12 well plates and incubated for 14 days. Cells were fixed and stained with crystal violet. (B) The number of colonies was quantified by using ImageJ software and the graph was plotted by using Graph pad Prism.

maximal inhibitory concentration (IC_{50}) values were calculated and are presented in Fig. 2B. *In vitro* cytotoxicity assays revealed that the carboranyl-BODIPY conjugates exhibited varying levels of toxicity against HeLa cervical cancer cells. Notably, ***o*-CB-10** demonstrated the highest cytotoxicity, with an IC_{50} value of 12.03 μM, indicating its potent anti-cancer activity. Conversely, ***m*-CB-15** displayed intermediate cytotoxicity (IC_{50} = 28.74 μM), while the phenylene BODIPY (**PB-20**) exhibited significantly lower cytotoxicity (IC_{50} = 48.35 μM). Surprisingly, the methylene-bridged *ortho*-carboranyl BODIPY conjugates, **Me-*o*-CB-28** and **Me-*o*-CB-35**, exhibited notably lower cytotoxicity, with IC_{50} values of 48.99 μM and 42.38 μM, respectively. These findings suggest that the conjugation of carborane moieties to BODIPY enhances cytotoxicity compared to phenylene-based conjugates with *ortho*-carborane showing greater potency than *meta*-carborane (Fig. 3). Furthermore, the presence of a methylene spacer between the carborane and BODIPY moieties appears to significantly diminish cytotoxicity, possibly due to disruption of the electronic conjugation between these groups.

2.2.2 Effect of BODIPY conjugates on HeLa cell proliferation. The anti-cancer effects of BODIPY conjugates can further be assessed form the inhibition of cell proliferation. The study

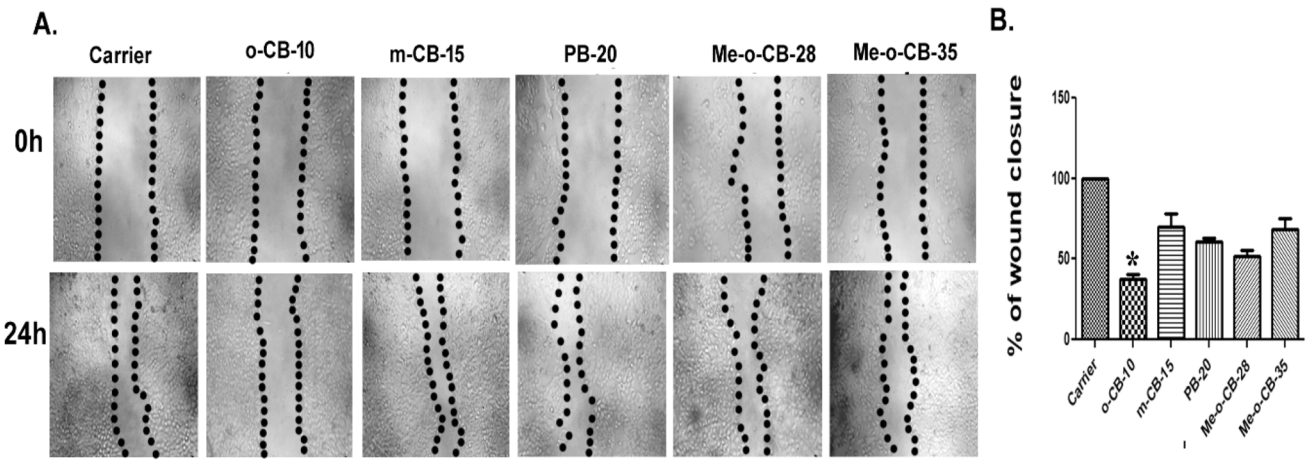

Fig. 5 (A) Photomicrograph of HeLa cells treated with carrier or 10 μM concentrations of each of the compounds at 0 h, and 24 h. (B) Graph represents the closure of wound area for carrier and compound treated cells at 0 h, and 24 h respectively. The compound ***o*-CB-10** has least wound closure than carrier and others. Statistical analysis was carried out using ANOVA and the $p < 0.05$.

evaluates the reproductive potential of cells for unrestricted division and colony formation by employing the cell survival assay to examine the capacity of an individual cell to develop into a colony.[96] HeLa Cells were treated with a fixed sub-lethal concentration (10 μM) of the BODIPY conjugates (***o*-CB-10**, ***m*-CB-15**, **PB-20**, **Me-*o*-CB-28** and **Me-*o*-CB-35**) along with the

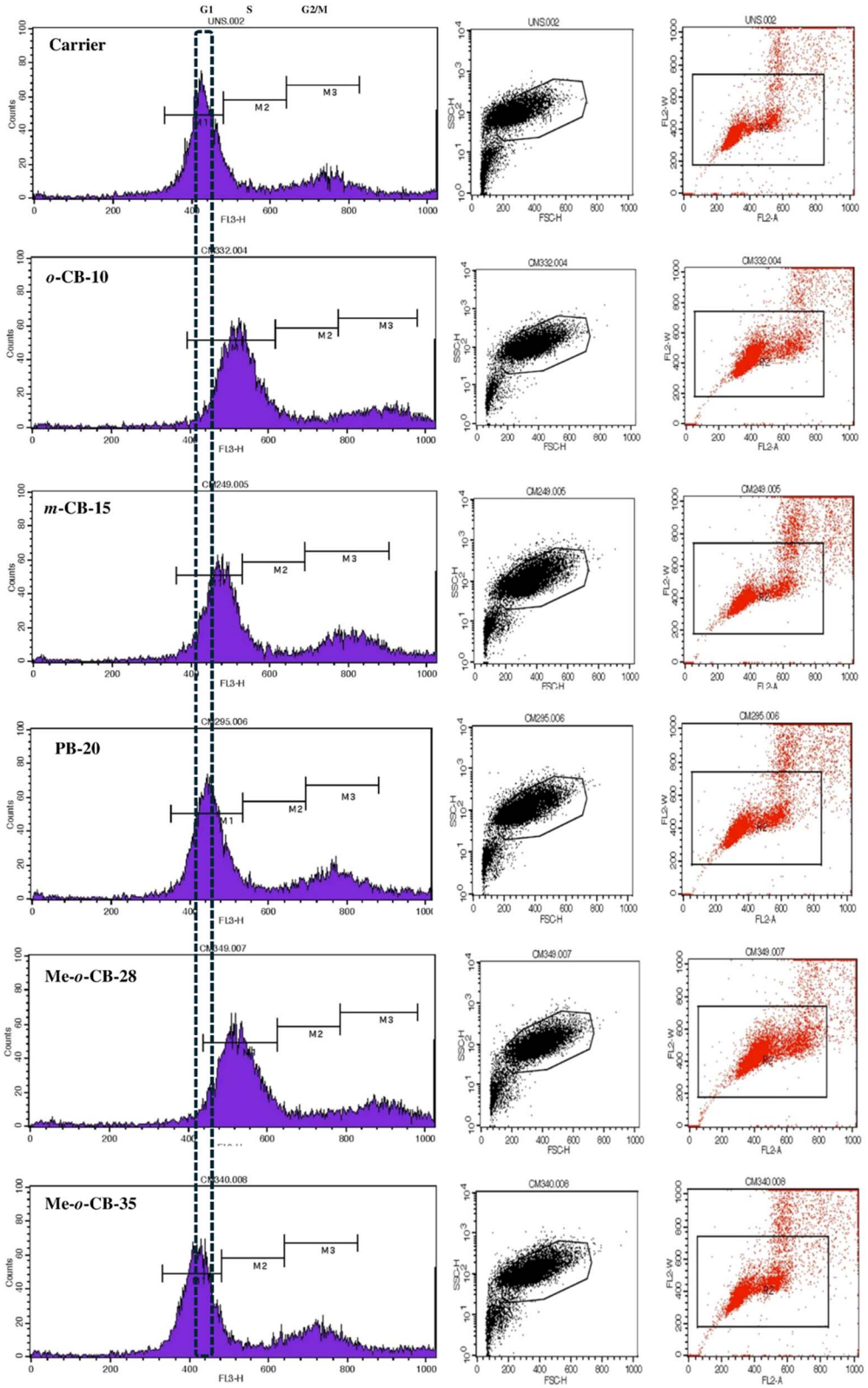

Fig. 6 Effect of BODIPY conjugates on the cell cycle distribution of HeLa cells. The compounds *o*-CB-10 and Me-*o*-CB-28 treated cell are arrested in S phase of cell cycle.

carrier. The colonies were stained with crystal violet, and the photograph was taken. The representative images of crystal violet stained colonies are shown in Fig. 4A. The colonies were counted and shown in graph Fig. 4B. The result indicates that ***o*-CB-10** is more effective in inhibiting HeLa cell proliferation compared to other tested compounds. Significant anti-proliferative activity was observed in the case of *ortho*-carboranyl BODIPY ***o*-CB-10**, while other compounds under study were found to be less efficient in inhibiting HeLa cell proliferation.

2.2.3 Effects of BODIPY conjugates on HeLa cell migration. The development of tumors to metastasis is a multistage process wherein malignant cells spread from the main tumor to inhabit distant locations.[97] To investigate the potential of BODIPY conjugates (***o*-CB-10**, ***m*-CB-15**, **Me-*o*-CB-28**, **Me-*o*-CB-35**, and **PB-20**) to inhibit cell migration, a wound-healing assay was employed. This *in vitro* model mimics the migratory behavior of cells observed *in vivo* during wound repair. By creating a "wound" in a cell monolayer and monitoring its closure over time, the rate of cell migration can be quantified. The wound was made using a P10 pipette tip and treated with carrier (DMSO) as well as 10 μM concentration of each of the synthesized BODIPY conjugates for 24 h. To observe the scratch, distance images were collected at 0 hours and 24 hours under an inverted microscope and are shown in Fig. 5A. Cell migration was analyzed as reported earlier[98] and plotted in graph as depicted in Fig. 5B. The result indicate that ***o*-CB-10** is highly significant in inhibiting cell migration in comparison to the carrier and other tested compounds.

2.2.4 Flow cytometry study of BODIPY conjugates. To investigate the effects of BODIPY conjugates on cell cycle regulation, HeLa cells were treated with a fixed sub-lethal concentration (10 μM) of each BODIPY conjugate for 24 hours. The percentage of cells in the G1, S, and G2/M phases of the cell cycle was determined based on the distribution of PI fluorescence intensity (FL2-A channel). Forward scatter (FSC–H) was used to exclude cell debris and aggregates. The results depicted in Fig. 6 demonstrate that treatment with ***o*-CB-10** and **Me-*o*-CB-28** induced a significant arrest of HeLa cells in the S phase of the cell cycle. In contrast, the remaining compounds, ***m*-CB-15**, **PB-20**, and **Me-*o*-CB-35**, primarily caused a G1 phase arrest. These findings suggest that the BODIPY conjugates exert distinct effects on cell cycle progression, with ***o*-CB-10** and **Me-*o*-CB-28** specifically targeting S phase cell cycle arrest. S phase arrest serves as a protective mechanism that facilitates DNA repair, prevents mutation accumulation, and enhances therapeutic strategies against cancer by promoting apoptosis and enabling synchronized cellular responses.[99]

2.2.5 Effects of BODIPY compounds on the expression of p53 on HeLa cells. p53, a crucial tumor suppressor, safeguards genomic integrity by regulating cell cycle, DNA repair and apoptosis. Activated by DNA damage, p53 halts the cell cycle for repair or initiates apoptosis to prevent cancerous cells from spreading.[100,101] HeLa cells typically contain wild-type p53 alleles alongside HPV (human papillomaviruses) DNA.[102] Research shows that HPV E6 can inhibit p53's transcriptional activity without degrading it, which is crucial for understanding how HPV contributes to cervical carcinogenesis.[103] The expression levels and activity of p53 can serve as biomarkers for predicting responses to therapies. Elevated p53 levels have been associated with increased sensitivity to treatments that induce apoptosis.[104] We evaluated the p53 expression of HeLa cells treated with BODIPY conjugates (10 μM) using immunocytochemistry. The cells were stained with Hoechst 33342, and fluorescence images were merged using the ImageJ program, as shown in Fig. 7A. The images were quantified using an ImageJ plotted graph, and statistical analysis was carried out using Graph pad Prism with a *p*-value of 0.05, as shown in Fig. 7B. The data reveal that p53 expression was significantly higher in the cells treated with **Me-*o*-CB-28**. However, the other drugs did not significantly alter the expression of p53 remarkably (Fig. 8).

3. Conclusion

In summary, four carboranyl-BODIPY conjugates (***o*-CB-10**, ***m*-CB-15**, **Me-*o*-CB-28**, and **Me-*o*-CB-35**) and one phenylene-BODIPY conjugate (**PB-20**) were synthesized. The anti-cancer efficacy of the synthesized compounds were evaluated against HeLa cervical cancer cells. Among them, *ortho*-carboranyl BODIPY compound **10** (***o*-CB-10**) exhibited higher cytotoxicity,

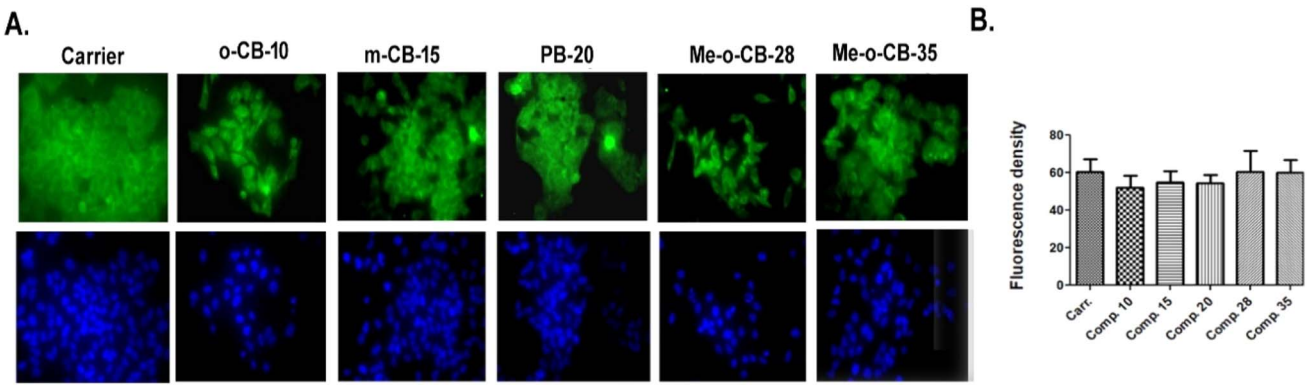

Fig. 7 p53 immunofluorescence analysis of HeLa cells treated with BODIPY conjugates. (A) Fluorescence images of the treated cells stained with Hoechst 33342 (B) statistical analysis using Graph pad Prism with *p* value 0.05.

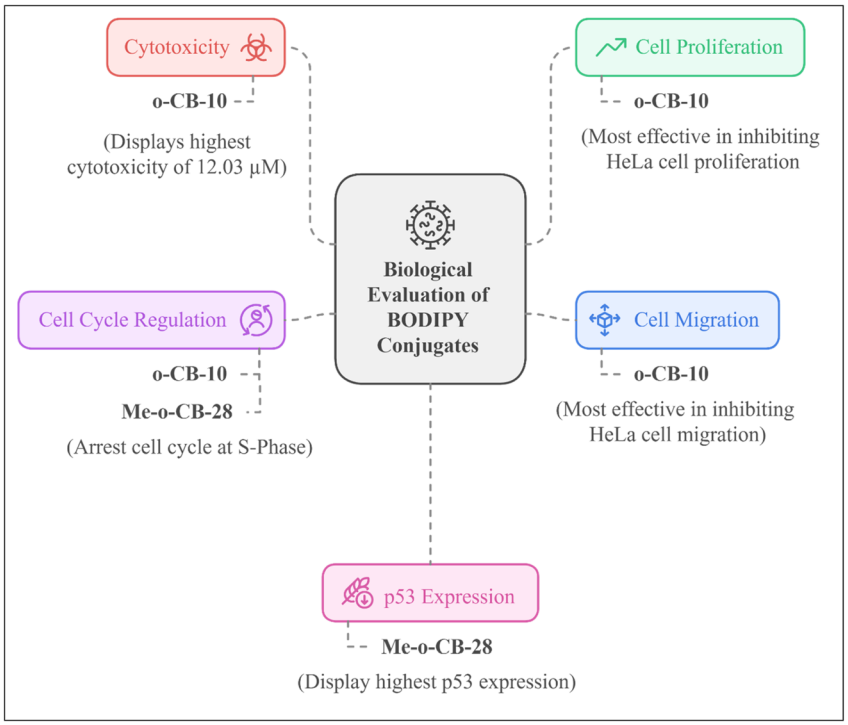

Fig. 8 Summary of biological evaluation of BODIPY conjugates.

efficiently inhibiting HeLa cell proliferation and migration, and causing cell cycle arrest at the S phase. The methylene-bridged *ortho*-carboranyl BODIPY conjugate **28** (**Me-*o*-CB-28**) was found to restore p53 protein in HeLa cells without affecting EGFR expression, while also inducing cell cycle arrest at the S phase, as shown by flow cytometry studies.

Although compound ***o*-CB-10** demonstrated potent anticancer activity, further studies are needed to clarify the underlying mechanisms of toxicity, particularly regarding the role of *ortho*-carborane. The observation that compounds **Me-*o*-CB-28**, which contain one *ortho*-carborane moiety and **Me-*o*-CB-35**, which contain two *ortho*-carborane moiety, do not exhibit proportionally greater toxicity suggests that factors such as cellular internalization or other mechanisms may influence the differences in cytotoxicity. Therefore, the role of *ortho*-carborane in the observed biological activity remains inconclusive.

These findings highlight the potential of carboranyl-BODIPY conjugates as anticancer agents. The effectiveness of the conjugates can be attributed to their ability to generate reactive oxygen species (ROS).[105] When the conjugates react chemically with cancer cells, the generated ROS can induce oxidative stress within cancer cells, leading to DNA damage, protein oxidation, and lipid peroxidation.[106] This oxidative stress can trigger apoptotic pathways, ultimately resulting in cell death. Moreover, the conjugates also interact with cellular targets involved in cell cycle regulation or signaling pathways, disrupting normal cellular processes and promoting apoptosis. The combined effects of these mechanisms contribute to the observed anticancer activity of the carboranyl-BODIPY conjugates. But further research involving other cancer cell lines, *in vivo* models, and mechanistic studies is required to better understand their efficacy, specificity, and potential side effects. Ongoing work is addressing these aspects.

4. Experimental section

4.1 Materials and methods

Reactions were generally performed under argon atmosphere in oven-dried flasks. Solvents and reagents were added using syringes. Solvents were dried and distilled using standard procedures. Reagents were purchased from commercial suppliers and were used as received without further purification. All compounds were purified by column chromatography on silica gel (60–120 mesh). Yields of the products refer to analytically pure samples. Progress of the reaction was monitored by TLC on silica gel 60 F_{254}-coated TLC plates and visualized by Short-UV light at 254 nm. ^{1}H and ^{13}C NMR spectra were recorded on Bruker Fourier Transform multinuclear NMR spectrometer at 400 MHz and 100 MHz respectively. Chemical shifts are reported relative to TMS (^{1}H: δ 0.00 ppm), $CDCl_3$ (^{13}C: $\delta = 77.0$ ppm) and coupling constants are given in Hertz (Hz). ^{11}B NMR spectra are proton-decoupled and recorded at 128 MHz relative to $BF_3 \cdot Et_2O$. ^{19}F NMR spectra were recorded at 376 MHz. FT-IR spectra were recorded on a Thermo Scientific Nicolet iS5 FT-IR spectrophotometer. Melting points were measured with optics digital melting point apparatus and are uncorrected.

4.2 Cell culture

Dulbecco's modified eagle medium (DMEM), fetal bovine serum (FBS), trypsin 0.25% EDTA, penicillin–streptomycin (cell

clone, Genetix India), ITS – Insulin Transferrin Selenium (cell clone). Human cervical cancer (HeLa cells) obtained from National Centre for Cell Sciences, Pune, India and were cultured in complete Dulbecco's modified eagle medium (DMEM) supplemented with 10% Fetal Bovine Serum (FBS) and 1% penicillin–streptomycin (PS) in a humidified incubator with 5% CO_2 and in atmospheric oxygen.

4.3 Cell viability assay

Cells were seeded in 96 well plates (2×10^3 per well) incubated overnight for attachment and treated with different concentrations (1.25 μM, 2.51 μM, 5.02 μM, 10.05 μM, 20.11 μM, 40.23 μM and 80 μM) of BODIPY conjugates (***o*-CB-10**, ***m*-CB-15**, **PB-20**, **Me-*o*-CB-28**, and **Me-*o*-CB-35**) for 72 h. Then 50 μl of 3-(4,5-dimethylthiazol-2-yl)-2,5-diphenyltetrazolium bromide (MTT) solution (5 mg mL^{-1} in DMEM w/o phenol red) was added to each well and the cells were further incubated for next 4 h. After that, the medium was aspirated, and the purple formazan crystals were dissolved by adding 80 μl DMSO and kept in a shaker for 30 minutes. Then absorbance was measured at 595 nm by a microplate reader.

4.4 Colony forming assay

Colony Forming Assay was performed by taking approximately 500 numbers of cells per well. They were seeded in a 12 well plate and treated with 10 μM concentrations of drugs and carrier. The next day the drug was discarded, and new complete media was added and was left for 14 days. The media was changed at regular intervals. After that we fixed the cells with methanol and acetic acid at 1 : 3 ratios and left it for 30 minutes. Then 200–300 μl of crystal violet was added for further 15 minutes and the plate was washed with tap water. The colony of cells was counted in bare eyes and the graph was plotted.

4.5 Wound healing assay

For wound healing assay cells were seeded in 12 well plates (10^5 cells per well) and incubated at 37 °C in 5% CO_2 incubator. After 24 hours of cell seeding, they were treated with 10 μM concentrations of synthetic compounds along with the carrier. Then a scratch wound was made on the confluent monolayer of HeLa cells with P10 pipette tip. Then the cells were observed under an inverted microscope at '0' hours and '24' hours and the image was captured. All the images were quantified using ImageJ and the graph was plotted by using GraphPad prism against wound size on the '*X*' axis and time on the '*Y*' axis.

4.6 Immunocytochemistry

Cells were cultured in 96 well plates and treated with carrier and respective BODIPY conjugated compounds (10 μM) for 24 h. The cells were fixed by 4% formaldehyde for 30 minutes, permeabilized using 0.25% Triton X-100, washed three times with ice-cold PBS each for 5 minutes. The cells were blocked with 1% BSA in PBST for 1 hour, incubated with diluted antibody (1 : 300 dilution) in blocking solution overnight at 4 °C. After overnight incubation, the cells were washed three times in PBS, 5 minutes in each wash, followed by incubated with diluted secondary antibody (1 : 300 dilution) for three hours at room temperature in dark and washed three times with PBS for 5 minutes each in dark. Nuclei were stained with diluted Hoechst solution for 30 minutes and images were taken in fluorescence microscope.

4.7 Flow cytometry

Subconfluent cells (4×10^5 no of cells) were incubated in 6 mm well plates for 24 h and treated with the carrier and respective BODIPY conjugated compound such 5 μM and 10 μM. After 24 h of treatment, the cells were harvested with Trypsin/EDTA, centrifuged for getting the plate. These plates were properly mixed with 75% ethanol for preservation. The cells were finally resuspended in PI solution (50 μL ml^{-1}) and Rnase A (10 mg mL^{-1}) and incubated for 30 min at 25 °C. Finally, the distribution of cells in various phases of the cell cycle was estimated using BD Accuri E6 flow cytometer at 10 000 cells.

4.8 Preparation and analytical data of compounds

4.8.1 Compound 3. Commercially available 1-bromo-4-iodobenzene **1** (3.0 g, 10.6 mmol) was dissolved in anhydrous THF (50 mL). To that solution triethylamine (6.0 mL), cuprous iodide (81 mg, 0.424 mmol), $PdCl_2(PPh_3)_2$ (149 mg, 0.212 mmol) and trimethyl silyl acetylene (1.47 mL, 10.6 mmol) were added and stirred at room temperature for 3 hours. The reaction mixture was filtered through short silica gel pad and evaporated. The crude product obtained was purified by silica gel column chromatography using hexane as eluent to obtain 2.5 g of pure compound **3** as colorless solid. Yield: 93%. Mp: 60 °C. ^{1}H NMR (400 MHz, $CDCl_3$, δ ppm): 7.24 (d, $J = 8.0$ Hz, 2H), 7.13 (d, $J = 8.0$ Hz, 2H), 0.05 (s, 9H, $-CH_3$). ^{13}C NMR (100 MHz, $CDCl_3$, δ ppm): 133.5, 131.6, 122.9, 122.2, 104.0, 95.7, 0.01. HRMS (*m*/*z*): calcd for $C_{11}H_{13}BrSi$: 251.9964, found 251.9961 [M^+].

4.8.2 Compound 4. To a solution of compound **3** (4.0 g, 15.79 mmol) in mixed solvents (80 mL) (THF : MeOH = 1 : 1), K_2CO_3 (3.27 g, 23.7 mmol) was added and stirred at room temperature for 3 hours. Filtered the reaction mixture over short silica pad and concentrated. The crude product was purified by silica gel column chromatography using hexane as eluent to obtain 2.2 g of pure compound **4** as a colorless solid. Yield: 77%. Mp: 65 °C. ^{1}H NMR (400 MHz, $CDCl_3$, δ ppm): 7.38 (d, $J = 8.0$ Hz, 2H), 7.27 (d, $J = 8.0$ Hz, 2H), 3.04 (s, 1H alkyne-H). ^{13}C NMR (100 MHz, $CDCl_3$, δ ppm): 133.6, 131.6, 123.2, 121.1, 82.6, 78.4. IR (KBr): 2924, 2853, 2108, 1484, 821 cm^{-1}. HRMS (*m*/*z*): calcd for C_8H_5Br: 180.9647, found 180.9646 [M^+].

4.8.3 Compound 5. Solution of decaborane (1.42 g, 11.6 mmol) in anhydrous CH_3CN (14 mL) was refluxed at 100 °C for 2 hours to obtain a white precipitate. To that precipitate compound **4** (1.4 g, 7.73 mmol) dissolved in anhydrous acetonitrile (5 mL) was added and refluxed at 100 °C for another 12 hours. After completion of reaction, MeOH (2 mL) was added to quench the excess decaborane and concentrated in rotary evaporator. The crude product was purified by silica gel column chromatography using hexane as eluent to obtain pure compound **5** as white solid. Yield: 65%. Mp: 135 °C. ^{1}H NMR (400 MHz, $CDCl_3$, δ ppm): 7.46 (d, $J = 8.0$ Hz, 2H), 7.34 (d, $J =$

12.0 Hz, 2H), 3.91 (s, 1H, C_{cage}–H). ^{13}C NMR (100 MHz, $CDCl_3$, δ ppm): 132.6, 132.1, 129.3, 124.7, 75.6 (C_{cage}–C), 60.2 (C_{cage}–C). ^{11}B NMR (128 MHz, $CDCl_3$, proton decoupled): −2.23, −3.39, −9.19, −10.39, −13.0. IR (KBr): 3063, 2958, 2921, 2565 (B–H), 1633, 1491, 1397, 1070, 830 cm^{-1}. HRMS (*m*/*z*): calcd for $C_8H_{15}B_{10}Br$: 298.1355, found 298.1344 [M^+].

4.8.4 Compound 7. To a solution of compound **5** (200 mg, 0.664 mmol) and 4-formylphenylboronic acid **6** (199 mg, 1.328 mmol) in anhydrous 1,4-dioxane (15 mL), Cs_2CO_3 (234 mg, 0.664 mmol) was added. Refluxed the reaction mixture at 100 °C for 15 hours. After completion of reaction, filtered the reaction mixture through short silica gel pad and concentrated. The crude product was purified by silica gel column chromatography using 10% ethyl acetate in hexane as eluent to obtain pure compound **7** as white solid. Yield: 51%. Mp: 170 °C. ^{1}H NMR (400 MHz, $CDCl_3$, δ ppm): 10.05 (s, 1H, –CHO), 7.96 (d, J = 8.0 Hz, 2H), 7.71 (d, J = 8.0 Hz 2H), 7.59 (s, 4H), 4.03 (s, 1H, C_{cage}–H). ^{13}C NMR (100 MHz, $CDCl_3$, δ ppm): 191.8, 145.3, 141.4, 135.9, 133.7, 130.5, 128.3, 127.8, 127.8, 76.1 (C_{cage}–C), 60.3 (C_{cage}–C). ^{11}B NMR (128 MHz, $CDCl_3$, proton decoupled): −2.31, −3.48, −9.19, −10.39, −12.41. IR (KBr): 3029, 2962, 2921, 2580 (B–H), 1693 (C═O), 1605, 1390, 1170, 1072, 1003, 820 cm^{-1}. HRMS (*m*/*z*): calcd for $C_{15}H_{20}B_{10}O$: 325.2590, found 325.2588 [M^+].

4.8.5 Compound 9. To a solution of compound **7** (200 mg, 0.613 mmol) and compound **8** (225 mg, 1.349 mmol) in anhydrous dichloromethane (20 mL),TFA (0.5 mL, 6.13 mmol) was added at 0 °C and stirred at room temperature for 2 hours. After completion of reaction, distilled water (10 mL) was added to quench the reaction. Extracted the crude product using dichloromethane, washed with water (3 times), dried the combined organic layers over anhydrous Na_2SO_4 and concentrated. The crude product was purified by silica gel column chromatography using 12% ethyl acetate in hexane as eluent to obtain 260 mg of pure compound **9** as white solid. Yield: 66%. Mp: 137 °C.^{1}H NMR (400 MHz, $CDCl_3$, δ ppm): 8.61 (s, 2H, –NH), 7.52 (d, J = 8.0 Hz, 4H), 7.47 (d, J = 8.0 Hz, 2H),7.16 (d, J = 8.0 Hz, 2H), 5.55 (s, 1H, *meso*-H), 4.21 (q, J = 8.0 Hz, 4H, –CH_{2ester}), 4.0 (s, 1H, C_{cage}–H), 2.23 (s, 6H, –$CH_{3pyrrole}$), 1.81 (s, 6H, –$CH_{3pyrrole}$), 1.29 (t, J = 8.0 Hz, 6H, –CH_{3ester}). ^{13}C NMR (100 MHz, $CDCl_3$, δ ppm): 162.1, 142.2, 139.3, 138.5, 132.6, 131.6, 129.0, 128.2, 127.7, 127.4, 118.2, 118.1, 76.4 (C_{cage}–C), 60.0, 53.5 (C_{cage}–C), 40.6 (*meso*-C), 14.6, 10.8, 9.0. ^{11}B NMR (128 MHz, $CDCl_3$, proton decoupled): −2.25, −3.57, −9.27, −10.64, −12.25. IR (KBr): 3307, 3054, 2978, 2924, 2858, 2594 (B–H), 1670, 1498, 1439, 1387, 1249, 1146, 1097, 944 cm^{-1}. HRMS (*m*/*z*): calcd for $C_{33}H_{44}B_{10}N_2O_4$: 641.4377, found 641.4375 [M^+].

4.8.6 Compound *o*-CB-10. To a solution of compound **9** (230 mg, 0.358 mmol) in anhydrous dichloromethane (30 mL), DDQ (98 mg, 0.429 mmol) was added and stirred at room temperature for 1 hour. After complete consumption of starting material **9** monitored by TLC, triethylamine (0.5 mL, 3.58 mmol) was added to it followed by $BF_3{\cdot}OEt_2$ (0.9 mL, 7.16 mmol) at 0 °C and stirred at room temperature for another 2 hours. After completion of reaction distilled water (10 mL) was added to the reaction mixture at 0 °C to quench the reaction. Extracted the crude product using dichloromethane (3 times). The combined organic layers were dried over anhydrous Na_2SO_4 and concentrated. The crude product was purified by neutral silica gel column chromatography using 15% ethyl acetate in hexane as eluent to obtain pure compound ***o*-CB-10** as red solid. Yield: 41%. Mp: 127 °C.^{1}H NMR (400 MHz, CD_2Cl_2, δ ppm): 7.61 (d, J = 8.0 Hz, 2H), 7.54 (d, J = 8.0 Hz, 2H), 7.51 (d, J = 8.0 Hz, 2H), 7.37 (d, J = 8.0 Hz, 2H), 4.13 (q, J = 8.0 Hz, 4H, –CH_{2ester}), 4.04 (s, 1H, C_{cage}–H), 2.15 (s, 6H, –$CH_{3pyrrole}$), 1.55 (s, 6H, –$CH_{3pyrrole}$), 1.32 (t, J = 8.0 Hz, 6H, –CH_{3ester}). ^{13}C NMR (100 MHz, CD_2Cl_2, δ ppm): 161.5, 141.4, 139.2, 133.6, 128.1, 128.1, 127.5, 127.4, 127.3, 127.2, 118.0, 117.6, 76.6 (C_{cage}–C), 74.4, 61.9 (C_{cage}–C), 59.9, 14.2, 10.2, 9.2. ^{11}B NMR (128 MHz, CD_2Cl_2, proton decoupled): 0.23 (t, J = 28.2 Hz, BF_2), −2.16, −8.94, −10.78(C_{cage}–B). ^{19}F NMR (376 MHz, CD_2Cl_2, δ ppm): −141.09 (q, J = 26.3 Hz). IR (KBr): 2925, 2854, 2595 (B–H), 1664, 1443, 1385, 1243, 1102, 1032, 818 cm^{-1}. HRMS (*m*/*z*): calcd for $C_{33}H_{41}B_{11}F_2N_2O_4$: 686.4125, found 686.4207 [M^+].

4.8.7 Compound 13. To a solution of compound **12** (500 mg, 1.66 mmol) in mixed solvents (THF : toluene = 1 : 1) (30 mL), 4-formylphenylboronic acid (498 mg, 3.32 mmol), $PdCl_2(PPh_3)_2$ (58 mg, 5 mol%), a solution of K_2CO_3 (687 mg, 4.98 mmol) in 3 mL of distilled water were added and refluxed at 110 °C for 24 hours. Extracted the crude product using dichloromethane (3 times), dried the combined organic layer over anhydrous Na_2SO_4 and concentrated. The crude product was purified by silica gel column chromatography using 5% ethyl acetate in hexane as eluent to obtain pure compound **13** as white solid. Yield: 63%. Mp: 140 °C.^{1}H NMR (400 MHz, $CDCl_3$, δ ppm): 9.98 (s, 1H, –CHO), 7.78 (d, J = 8.0 Hz, 2H), 7.63 (d, J = 8.0 Hz, 2H), 7.50 (s, 4H), 3.03 (s, 1H, C_{cage}–H). ^{13}C NMR (100 MHz, $CDCl_3$, δ ppm): 191.8, 145.8, 140.1, 135.6, 135.4, 130.3, 128.5, 127.6, 127.3, 76.7 (C_{cage}–C), 55.2 (C_{cage}–C). ^{11}B NMR (128 MHz, $CDCl_3$, proton decoupled): −3.79, −10.31, −13.29, −15.15. IR (KBr): 3061, 2959, 2926, 2851, 2734, 2604 (B–H), 1701 (C═O), 1605, 1492, 1215, 1170, 1005, 838 cm^{-1}. HRMS (*m*/*z*): calcd for $C_{15}H_{20}B_{10}O$: 325.2599, found 325.2587 [M^+].

4.8.8 Compound 14. To a solution of compound **13** (250 mg, 0.766 mmol) and compound **8** (281 mg, 1.687 mmol) in anhydrous dichloromethane (30 mL), TFA (0.23 mL, 3.064 mmol) was added at 0 °C and stirred at room temperature for 4 hours. After completion of reaction, quenched the reaction using distilled water. Extracted the crude product using dichloromethane (3 times), washed with water, dried the combined organic layers over anhydrous Na_2SO_4 and concentrated. The crude product was purified by silica gel column chromatography using 7% ethyl acetate in hexane as eluent to obtain pure compound **14** as colorless solid. Yield: 85%. Mp: 92 °C.^{1}H NMR (400 MHz, CD_2Cl_2, δ ppm): 8.86 (s, 2H, –NH), 7.36–7.42 (dd, J = 8.0 Hz, 6H), 7.07 (d, J = 8.0 Hz, 2H), 5.55 (s, 1H, *meso*-H), 4.07 (q, J = 8.0 Hz, 4H, –CH_{2ester}), 3.09 (s, 1H, C_{cage}–H), 2.11 (s, 6H, –$CH_{3pyrrole}$), 1.76 (s, 6H, –$CH_{3pyrrole}$), 1.16 (t, J = 8.0 Hz, 6H, –CH_{3ester}). ^{13}C NMR (100 MHz, CD_2Cl_2, δ ppm): 161.8, 140.8, 139.4, 138.5, 134.2, 131.8, 128.7, 128.3, 127.3, 126.8, 118.2, 118.0, 78.2 (C_{cage}–C), 59.8, 55.5 (C_{cage}–C), 40.2 (*meso*-C), 14.2, 10.4, 8.6. ^{11}B NMR (128 MHz, CD_2Cl_2, proton decoupled): −2.36, −3.5, −9.27, −10.53, −11.04, −12.38. IR (KBr): 3310 (N–H), 3032, 2924, 2832, 2740, 2598 (B–H), 1696,

1604, 1520, 1483, 1393, 1306, 1213, 1167, 1005, 840 cm^{-1}. HRMS (*m*/*z*): calcd for $C_{33}H_{44}B_{10}N_2O_4$: 641.4262, found 641.4376 [M^+].

4.8.9 Compound *m*-CB-15. To a solution of compound **14** (250 mg, 0.389 mmol) in anhydrous dichloromethane (30 mL), DDQ (97 mg, 0.428 mmol) was added and stirred at room temperature for 1 hour. After complete consumption of starting material **14** checked by TLC, triethylamine (0.27 mL, 1.945 mmol) was added to the reaction mixture followed by $BF_3 \cdot OEt_2$ (0.49 mL, 3.89 mmol) at 0 °C and stirred at room temperature for another 2 hours. After completion of reaction, quenched the reaction by using distilled water (10 mL) at 0 °C and extracted with dichloromethane (3 times). Combined organic layers were dried over anhydrous Na_2SO_4 and concentrated. The crude product was purified by neutral silica gel column chromatography using 10% ethyl acetate in hexane as eluent to obtain pure compound ***m*-CB-15** as red solid. Yield: 38%. Mp: 230 °C.^{1}H NMR (400 MHz, CD_2Cl_2, δ ppm): 7.70 (d, J = 8.0 Hz, 2H), 7.53 (d, J = 8.0 Hz, 2H), 7.47 (d, J = 8.0 Hz, 2H), 7.28 (d, J = 8.0 Hz, 2H), 4.33 (q, J = 8.0 Hz, 4H, $-CH_{2ester}$), 3.11 (s, 1H, C_{cage}–H), 1.90 (s, 6H, $-CH_{3pyrrole}$), 1.31 (s, 6H, $-CH_{3pyrrole}$), 1.31 (t, J = 8.0 Hz, 6H, $-CH_{3ester}$). ^{13}C NMR (100 MHz, CD_2Cl_2, δ ppm): 162.1, 141.1, 140.2, 135.0, 133.9, 133.0, 128.5, 128.3, 128.0, 127.0, 118.0, 117.5, 78.0 (C_{cage}–C), 59.9, 55.5 (C_{cage}–C), 31.9, 13.8, 12.2, 9.2. ^{11}B NMR (128 MHz, CD_2Cl_2, proton decoupled): 0.23 (t, J = 29.4 Hz, BF_2), −3.93, −10.43, −13.27, −15.07(C_{cage}–B). ^{19}F NMR (376 MHz, CD_2Cl_2, δ ppm): −141.09 (q, J = 26.3 Hz). IR (KBr): 3060, 2926, 2848, 2604 (B–H), 1719, 1670, 1647, 1530, 1443, 1392, 1267, 1183, 1121, 1075, 1005 cm^{-1}. HRMS (*m*/*z*): calcd for $C_{33}H_{41}B_{11}F_2N_2O_4$: 686.4125, found 686.4106 [M^+].

4.8.10 Compound 17. To a solution of commercially available 1-bromo-4-iodobenzene **1** (1.5 g, 5.3 mmol) in mixed solvents (toluene : ethanol = 3 : 1) (20 mL), phenylboronic acid (646 mg, 5.3 mmol), $PdCl_2(PPh_3)_2$ (149 mg, 4 mol%), a solution of K_2CO_3 in distilled water (2 mL) were added and refluxed at 100 °C for 12 hours. Extracted the crude product using dichloromethane (3 times). Dried the combined organic layers were over anhydrous Na_2SO_4 and concentrated. The crude product was purified by silica gel column chromatography using hexane as eluent to obtain pure compound **17** as white solid. Yield: 81%. Mp: 92 °C.^{1}H NMR (400 MHz, $CDCl_3$, δ ppm): 7.51 (d, J = 8.0 Hz, 2H), 7.45–7.48 (dd, J = 8.0 Hz, 2H), 7.33–7.37 (m, J = 8.0 Hz, 4H), 7.27 (t, J = 8.0, Hz, 1H). ^{13}C NMR (100 MHz, $CDCl_3$, δ ppm): 131.9, 129.0, 128.8, 127.7, 127.3, 127.2, 127.0, 121.6. HRMS (*m*/*z*): calcd for $C_{12}H_9Br$: 233.1039, found 250.82 [$M^+ + H_2O$].

4.8.11 Compound 18. To a solution of compound **17** (700 mg, 3.0 mmol) in mixed solvents (THF : toluene = 1 : 1) (40 mL), 4-formylphenylboronic acid **6** (675 mg, 4.5 mmol), $PdCl_2(PPh_3)_2$ (84 mg, 4 mol%), a solution of K_2CO_3 (1.24 g, 9.0 mmol) in distilled water (2 mL) were added and refluxed at 110 °C for 24 hours. Extracted the crude product using dichloromethane (3 times). Dried the combined organic layers were over anhydrous Na_2SO_4 and concentrated. The crude product was purified by silica gel column chromatography using 10–20% ethyl acetate in hexane as eluent to obtain pure compound **18** as white solid. Yield: 65%. Mp: > 200 °C.^{1}H NMR (400 MHz, $CDCl_3$, δ ppm): 9.98 (s, 1H, –CHO), 7.89 (d, J = 8.0 Hz, 2H), 7.72 (d, J = 8.0 Hz, 2H), 7.64 (s, 4H), 7.57 (d, J = 8.0 Hz, 2H), 7.39 (t, J = 8.0 Hz, 2H), 7.30 (t, J = 8.0 Hz, 1H). ^{13}C NMR (100 MHz, $CDCl_3$, δ ppm): 192.0, 146.7, 141.4, 140.3, 138.5, 135.2, 130.4, 128.9, 127.8, 127.8, 127.7, 127.6, 127.1. IR (KBr): 2921, 2831, 2741, 1703 (C═O), 1602, 1483, 1385, 1005, 820 cm^{-1}. FTMS (*m*/*z*): calcd for $C_{19}H_{14}O$: 258.3139, found 259.11 [M^+ + H].

4.8.12 Compound 19. To a solution of compound **18** (350 mg, 1.35 mmol) and **8** (497 mg, 2.98 mmol)in anhydrous dichloromethane (30 mL), TFA (1.0 mL, 13.5 mmol) was added at 0 °C and stirred at room temperature for 4 hours. After completion of reaction monitored by TLC, distilled water (10 ML) was added to quench the reaction. Extracted the crude product using dichloromethane (3 times). Dried the combined organic layers were over anhydrous Na_2SO_4 and concentrated. The crude product was purified by silica gel column chromatography using 10% ethyl acetate in hexane as eluent to obtain 500 mg of pure compound **19** as white solid. Yield: 64%. Mp: 197 °C.^{1}H NMR (400 MHz, CD_2Cl_2, δ ppm): 9.26 (s, 2H, –NH), 7.57 (dd, J = 8.0 Hz, 6H), 7.46 (d, J = 8.0 Hz, 2H), 7.36 (t, J = 8.0 Hz, 2H), 7.26 (t, J = 8.0 Hz, 1H), 7.09 (d, J = 8.0 Hz, 2H), 5.56 (s, 1H, *meso*-H), 4.03 (q, J = 8.0 Hz, 4H, $-CH_{2ester}$), 2.10 (s, 6H, $-CH_{3pyrrole}$), 1.80 (s, 6H, $-CH_{3pyrrole}$), 1.14 (t, J = 8.0 Hz, 6H, $-CH_{3ester}$). ^{13}C NMR (100 MHz, CD_2Cl_2, δ ppm): 162.0, 140.5, 140.1, 139.3, 139.2, 128.9, 128.7, 127.4, 127.3, 127.1, 126.9, 118.2, 118.0, 59.9, 40.0 (*meso*-C), 14.3, 10.5, 8.7. IR (KBr): 3349 (N–H), 2983, 2921, 2856, 1666, 1485, 1432, 1280, 1250, 1164, 1097, 761 cm^{-1}. HRMS (*m*/*z*): calcd for $C_{37}H_{38}N_2O_4$: 574.7086, found 573.34 [M^+ − H].

4.8.13 Compound PB-20. To a solution of compound **19** (330 mg, 0.574 mmol) in anhydrous dichloromethane (30 mL), DDQ (156 mg, 0.688 mmol) and stirred at room temperature for 2 hours. After complete consumption of starting material **19** checked by TLC, triethylamine (0.4 mL, 2.87 mmol) was added to it followed by $BF_3 \cdot OEt_2$ (0.7 mL, 5.74 mmol) at 0 °C and stirred at room temperature for another 2 hours. Quenched the reaction using distilled water (10 mL) at 0 °C and extracted the crude product using dichloromethane (3 times). Dried the combined organic layers were over anhydrous Na_2SO_4 and concentrated. The crude product was purified by silica gel column chromatography using 10% ethyl acetate in hexane as eluent to obtain pure compound **PB-20** as red solid. Yield: 42%. Mp: 110 °C.^{1}H NMR (400 MHz, CD_2Cl_2, δ ppm): 7.62 (s, 4H), 7.57–7.60 (m, J = 8.0 Hz, 4H), 7.38 (t, J = 8.0 Hz, 4H), 7.29 (d, J = 8.0 Hz, 1H), 4.14 (q, J = 8.0 Hz, 4H, $-CH_{2ester}$), 2.17 (s, 6H, $-CH_{3pyrrole}$), 1.58 (s, 6H, $-CH_{3pyrrole}$), 1.22 (t, J = 8.0 Hz, 6H, $-CH_{3ester}$). ^{13}C NMR (100 MHz, CD_2Cl_2, δ ppm): 161.5, 141.4, 140.5, 140.4, 140.3, 139.1, 128.8, 127.4, 127.4, 127.3, 127.1, 126.9, 118.0, 117.5, 74.5, 59.9, 14.2, 10.2, 9.3. ^{11}B NMR (128 MHz, CD_2Cl_2, proton decoupled): 0.25 (t, J = 28.2 Hz). ^{19}F NMR (376 MHz, CD_2Cl_2, δ ppm): −141.09 (q, J = 26.3 Hz). IR (KBr): 3023, 2926, 2864, 1669, 1645, 1484, 1445, 1268, 1187, 765 cm^{-1}. HRMS (*m*/*z*): calcd for $C_{37}H_{35}BF_2N_2O_4$: 621.2731, found 621.2727 [M^+].

4.8.14 Compound 23. To a solution of commercially available methyl-4-hydroxybenzoate **21** (1.5 g, 9.86 mmol) in anhydrous acetone (30 mL), K_2CO_3 (2.99 g, 21.67 mmol), propargyl bromide **22** (1.05 mL, 11.8 mmol) were added and refluxed at

60 °C for 24 hours. After completion of reaction, the reaction mixture was filtered through short silica gel pad and concentrated. The crude product was purified by silica gel column chromatography using 10% ethyl acetate in hexane as eluent to obtain 1.6 g of pure compound **23** as colorless solid. Yield: 86%. Mp: 78 °C.^{1}H NMR (400 MHz, $CDCl_3$, δ ppm): 7.99 (d, J = 8.0 Hz, 2H), 6.98 (d, J = 8.0 Hz, 2H), 4.73 (s, 2H, –CH_2), 3.87 (s, 3H, –CH_{3ester}), 2.54 (t, J = 4.0 Hz, 1H, alkyne-H). ^{13}C NMR (100 MHz, $CDCl_3$, δ ppm): 166.7, 161.2, 131.6, 123.5, 114.6, 77.9, 76.2, 55.9, 52.0. IR (KBr): 3246, 2958, 2913, 2860, 2128, 1706, 1608, 1511, 1440, 1289, 1176, 1106, 1024, 853 cm^{-1}. HRMS (m/z): calcd for $C_{11}H_{10}O_3$: 190.1953, found 191.05 [M^+ + H].

4.8.15 Compound 24. $LiAlH_4$ (1.59 g, 42.0 mmol) was suspended in dry THF (40 mL) and the reaction flask was cooled to 0 °C. Then compound **23** (2 g, 10.5 mmol) was dissolved in 10 mL of dry THF and added to the reaction mixture at 0 °C. The reaction mixture was stirred at 0 °C for 1 hour and then stirred at room temperature for another 4 hours. At 0 °C, water was added dropwise to the reaction mixture to quench the $LiAlH_4$, and reaction mixture was extracted with dichloromethane. The organic layers were washed with water, dried over anhydrous Na_2SO_4 and solvent was evaporated in rotary evaporator. The crude reaction mixture was purified by silica gel column chromatography using 30% ethyl acetate in hexane to obtain 1.4 g of compound **24** as colorless liquid. Yield: 82%. ^{1}H NMR (400 MHz, $CDCl_3$, δ ppm): 7.28 (d, J = 8.0 Hz, 2H), 6.95 (d, J = 8.0 Hz, 2H), 4.68 (d, J = 4.0 Hz, 2H, –CH_2), 4.59 (s, 1H, –OH), 2.51 (t, J = 4.0 Hz, 1H, alkyne-H). ^{13}C NMR (100 MHz, $CDCl_3$, δ ppm): 157.2, 134.2, 128.7, 115.1, 78.6, 75.7, 65.0, 55.9. IR (KBr): 3287, 2924, 2872, 2120, 1883, 1610, 1587, 1510, 1456, 1376, 1216, 1027, 814 cm^{-1}.

4.8.16 Compound 25. To a solution of compound **24** (1 g, 6.749 mmol) in anhydrous dichloromethane (40 mL), PCC (2.9 g, 13.489 mmol) was added at 0 °C and stirred at room temperature for 1 hour. Filtered the reaction mixture through short silica gel pad and concentrated. The crude product was purified by silica gel column chromatography using 15% ethyl acetate in hexane as eluent to obtain 850 mg of pure compound **25** as colourless solid. Yield: 79%. Mp: 90 °C.^{1}H NMR (400 MHz, $CDCl_3$, δ ppm): 9.87 (s, 1H, –CHO), 7.83 (d, J = 8.0 Hz, 2H), 7.06 (d, J = 8.0 Hz, 2H), 4.76 (d, J = 4.0 Hz, 2H, –CH_2), 2.56 (t, J = 4.0 Hz, 1H, alkyne-H). ^{13}C NMR (100 MHz, $CDCl_3$, δ ppm): 190.8, 162.4, 132.0, 130.7, 115.3, 77.6, 76.5, 56.0 IR (KBr): 3211, 3057, 2929, 2832, 2122, 1681 (C=O), 1603, 1577 cm^{-1}. HRMS (m/z): calcd for $C_{10}H_8O_2$: 161.0597, found 161.0596 [M^+].

4.8.17 Compound 26. To a solution of compound **25** (400 mg, 2.497 mmol) and compound **8** (915.65 mg, 5.49 mmol) in anhydrous dichloromethane (30 mL), TFA (3.8 mL, 49.94 mmol) was added at 0 °C and stirred at room temperature for 2 hours. After completion of reaction, quenched the reaction at 0 °C using distilled water (10 mL). Extracted the crude product using dichloromethane (3 times), washed with water, dried the combined organic layers over anhydrous Na_2SO_4 and concentrated. The crude product was purified by silica gel column chromatography using 10% ethyl acetate in hexane to obtain 758 mg of pure compound **26** as colorless solid. Yield: 64%. Mp: 100 °C. ^{1}H NMR (400 MHz, $CDCl_3$, δ ppm): 8.52 (s, 2H, –NH), 7.0 (d, J = 8.0 Hz, 2H), 6.89 (d, J = 8.0 Hz, 2H), 5.46 (s, 1H, *meso*-H), 4.65 (s, 2H, –CH_2), 4.20 (q, J = 8.0 Hz, 4H, –CH_{2ester}), 2.52 (t, J = 4.0 Hz, 1H_{alkyne}), 2.23 (s, 6H, –$CH_{3pyrrole}$), 1.78 (s, 6H, –$CH_{3pyrrole}$), 1.28 (t, J = 8.0 Hz, 6H, –CH_{3ester}). ^{13}C NMR (100 MHz, $CDCl_3$, δ ppm): 162.0, 156.9, 132.1, 132.1, 129.4, 127.7, 118.0, 117.9, 115.4, 78.5, 75.8, 59.9, 55.9, 40.1 (*meso*-C), 14.6, 10.7, 8.9. IR (KBr): 3284 (N–H), 2978, 2924, 2860, 2120, 1652, 1508, 1441, 1245, 1146, 1099, 1026 cm^{-1}. HRMS (m/z): calcd for $C_{28}H_{32}N_2O_5$: 477.2384, found 477.2386 [M^+].

4.8.18 Compound 27. Solution of decaborane (205 mg, 1.678 mmol) in anhydrous acetonitrile (3 mL) and resulting solution was refluxed at 100 °C for 2 hours. To it a solution of compound **26** (400 mg, 0.839 mmol) in anhydrous acetonitrile (5 mL) was added and refluxed at 100 °C for another 12 hours. After completion of reaction, MeOH (2 mL) was added to quench the excess decaborane and concentrated. The crude product was purified by silica gel column chromatography using 15% ethyl acetate in hexane to obtain 300 mg of compound **27** as white solid. Yield: 60%. Mp: 156 °C. ^{1}H NMR (400 MHz, $CDCl_3$, δ ppm): 8.44 (s, 2H, –NH), 7.01 (d, J = 8.0 Hz, 2H), 6.76 (d, J = 8.0 Hz, 2H), 5.45 (s, 1H, *meso*-H), 4.38 (s, 2H, –CH_2), 4.23 (q, J = 8.0 Hz, 4H, –CH_{2ester}), 4.08 (s, 1H, C_{cage}-H), 2.23 (s, 6H, –$CH_{3pyrrole}$), 1.76 (s, 6H, –$CH_{3pyrrole}$), 1.30 (t, J = 8.0 Hz, 6H, –CH_{3ester}). ^{13}C NMR (100 MHz, $CDCl_3$, δ ppm): 162.0, 156.3, 133.4, 131.7, 129.8, 127.7, 118.1, 117.9, 115.3, 71.4 (C_{cage}–C), 69.3, 60.0, 57.8 (C_{cage}–C), 40.3 (*meso*-C), 14.6, 10.8. ^{11}B NMR (128 MHz, $CDCl_3$, proton decoupled): −3.10, −4.29, −9.38, −10.56, −11.91, −13.19. IR (KBr): 3322 (N–H), 2983, 2921, 2860, 2585 (B–H), 1678, 1655, 1508, 1441, 1241, 1142, 1021, 911 cm^{-1}. HRMS (m/z): calcd for $C_{28}H_{42}B_{10}N_2O_5$: 595.4170, found 595.4179 [M^+].

4.8.19 Compound Me-*o*-CB-28. To a solution of compound **27** (200 mg, 0.343 mmol) in anhydrous dichloromethane (20 mL), DDQ (117 mg, 0.514 mmol) was added at 0 °C and stirred at room temperature for 2 hours. Then after complete consumption of compound **27** checked by TLC, triethylamine (0.24 mL, 1.715 mmol) was added to it followed by $BF_3 \cdot OEt_2$ (0.43 mL, 3.43 mmol) at 0 °C and stirred at room temperature for another 2 hours. The reaction was quenched using distilled water (10 mL) at 0 °C and extracted the crude product using dichloromethane (3 times). Dried the combined organic layers were over anhydrous Na_2SO_4 and concentrated. The crude product was purified by neutral silica gel column chromatography using 20% ethyl acetate in hexane as eluent to obtain 85 mg of pure compound **Me-*o*-CB-28** as red solid. Yield: 39%. Mp: > 200 °C. ^{1}H NMR (400 MHz, CD_2Cl_2, δ ppm): 7.20 (d, J = 8.0 Hz, 2H), 7.02 (d, J = 8.0 Hz, 2H), 4.51 (s, 2H, –CH_2), 4.39 (q, J = 8.0 Hz, 4H, –CH_{2ester}), 4.16 (s, 1H, C_{cage}–H), 1.96 (s, 6H, –$CH_{3pyrrole}$),1.37 (t, J = 8.0 Hz, 6H, –CH_{3ester}), 1.34 (s, 6H, –$CH_{3pyrrole}$). ^{13}C NMR (100 MHz, CD_2Cl_2, δ ppm): 162.2, 158.2, 147.9, 145.2, 142.3, 133.3, 129.4, 129.1, 128.4, 115.8, 71.6 (C_{cage}–C), 69.1, 62.0, 58.5 (C_{cage}–C), 13.9, 12.4, 9.3. ^{11}B NMR (128 MHz, CD_2Cl_2, proton decoupled): −0.80 (t, J = 28.2 Hz, BF_2), −3.14, −4.36, −9.54, −10.71, −13.19(C_{cage}–B). ^{19}F NMR (376 MHz, CD_2Cl_2, δ ppm): −141.06 (q, J = 26.3 Hz). IR (KBr): 3081, 2980, 2925, 2570 (B–H), 1747, 1713, 1610, 1537, 1470, 1387, 1225,

1181, 1118, 1014, 856 cm^{-1}. HRMS (*m*/*z*): calcd for $C_{28}H_{39}B_{11}N_2F_2O_5$: 640.3918, found 640.4022 [M^+].

4.8.20 Compound 32. To a solution of compound **31** (1 g, 4.625 mmol) in anhydrous dichloromethane (40 mL), PCC (1.99 g, 9.25 mmol) was added at 0 °C and stirred at room temperature for 1 hour. Filtered the reaction mixture through short silica gel pad and concentrated. The crude product was purified by silica gel column chromatography using 15% ethyl acetate in hexane as eluent to obtain 840 mg of pure compound **32** as colorless solid. Yield: 85%. Mp: 70 °C.^{1}H NMR (400 MHz, $CDCl_3$, δ ppm): 9.89 (s, 1H, –CHO), 7.10 (d, $J = 0$ Hz, 2H), 6.84 (t, $J = 4.0$ Hz, 1H), 4.71 (d, $J = 0$ Hz, 4H, $-CH_2$), 2.54 (t, $J = 4.0$ Hz, 2H, alkyne-H). ^{13}C NMR (100 MHz, $CDCl_3$, δ ppm): 191.6, 159.2, 138.5, 109.0, 108.8, 77.8, 76.3, 56.2. IR (KBr): 2936, 2872, 2754, 2114, 1702 (C═O), 1601, 1459, 1340, 1280, 1155, 1061, 953, 895. HRMS (*m*/*z*): calcd for $C_{13}H_{10}O_3$: 215.0703, found 215.0702 [M^+].

4.8.21 Compound 33. To a solution of compound **32** (600 mg, 2.801 mmol) and **8** (1.03 g, 6.162 mmol) in anhydrous dichloromethane (40 mL), TFA (2.14 mL, 28.01 mmol) was added at 0 °C and stirred at room temperature for 2 hours. After completion of reaction, distilled water (10 mL) was added to quench the reaction. Extracted the crude product using dichloromethane, washed with water (3 times), dried the combined organic layers over anhydrous Na_2SO_4 and concentrated. The crude product was purified by silica gel column chromatography using 20–30% ethyl acetate in hexane to obtain 1.0 g of pure compound **33** as light pink solid. Yield: 67%. Mp: 155 °C. ^{1}H NMR (400 MHz, $CDCl_3$, δ ppm): 8.49 (s, 2H, –NH), 6.52 (t, $J = 4.0$ Hz, 1H), 6.34 (d, $J = 0$ Hz, 2H), 5.42 (s, 1H, *meso*-H), 4.59 (d, $J = 0$ Hz, 4H, $-CH_2$), 4.21 (q, $J = 8.0$ Hz, 4H, $-CH_{2ester}$), 2.52 (t, $J = 4.0$ Hz, $2H_{alkyne}$–H), 2.23 (s, 6H, $-CH_{3pyrrole}$), 1.78 (s, 6H, $-CH_{3pyrrole}$), 1.29 (t, $J = 8.0$ Hz, 6H, $-CH_{3ester}$). ^{13}C NMR (100 MHz, $CDCl_3$, δ ppm): 161.9, 159.1, 141.7, 131.3, 127.7, 118.1, 118.1, 108.4, 101.1, 78.1, 76.1, 60.0, 56.0, 41.2 (*meso*-C), 14.6, 10.8, 8.9. IR (KBr): 3320 (N–H), 2974, 2924, 2868, 2118, 1651, 1597, 1441, 1260, 1150, 1065, 943, 824, 776 cm^{-1}. HRMS (*m*/*z*): calcd for$C_{31}H_{34}N_2O_6$: 531.2490, found 531.2483 [M^+].

4.8.22 Compound 34. Solution of decaborane (461 mg, 3.769 mmol) in anhydrous acetonitrile (5 mL) was refluxed at 100 °C for 2 hours to obtain a white precipitate. To it a solution of compound **33** (500 mg, 0.942 mmol) in anhydrous acetonitrile (6 mL) was added and refluxed at 100 °C for another 16 hours. After completion of reaction, MeOH (2 mL) was added to quench the excess decaborane and concentrated. The crude product was purified by silica gel column chromatography using 15% ethyl acetate in hexane to obtain 530 mg of pure compound **34** as white solid. Yield: 73%. Mp: >200 °C.^{1}H NMR (400 MHz, $CDCl_3$, δ ppm): 8.43 (s, 2H, –NH), 6.25 (d, $J = 0$ Hz, 2H), 6.23 (t, $J = 4.0$ Hz, 1H), 5.41 (s, 1H, *meso*-H), 4.32 (s, 4H, $-CH_2$), 4.23 (q, $J = 8.0$ Hz, 4H, $-CH_{2ester}$), 3.99 (s, 2H, C_{cage}–H), 2.24 (s, 6H, $-CH_{3pyrrole}$), 1.78 (s, 6H, $-CH_{3pyrrole}$), 1.31 (t, $J = 8.0$ Hz, 6H, $-CH_{3ester}$). ^{13}C NMR (100 MHz, $CDCl_3$, δ ppm): 162.2, 158.7, 143.1, 130.7, 127.7, 118.5, 118.2, 108.6, 100.8, 71.4 (C_{cage}–C), 69.2, 60.2, 58.0 (C_{cage}–C), 41.1 (*meso*-C), 14.6, 10.8. ^{11}B NMR (128 MHz, CD_2Cl_2, proton decoupled): −2.95, −4.13, −9.34, −10.52, −13.13. IR (KBr): 3336 (N–H), 3048, 2980, 2926, 2852, 2593 (B–H), 1698, 1648, 1596, 1442, 1384, 1266, 1164, 1092, 1018, 944 777 cm^{-1}. HRMS (*m*/*z*): calcd for $C_{31}H_{54}B_{20}N_2O_6$: 767.6079, found 767.6077 [M^+].

4.8.23 Compound Me-*o*-CB-35. To a solution of compound **34** (400 mg, 0.5194 mmol) in anhydrous dichloromethane (30 mL), DDQ (130 mg, 0.571 mmol) was added at 0 °C and stirred at room temperature for 2 hours. After complete consumption of compound **34** checked by TLC, triethylamine (0.36 mL, 2.597 mmol) was added to it followed by $BF_3 \cdot OEt_2$ (0.65 mL, 5.194 mmol) at 0 °C and stirred at room temperature for another 2 hours. The reaction was quenched using distilled water (10 mL) at 0 °C and extracted the crude product using dichloromethane (3 times). Dried the combined organic layers were over anhydrous Na_2SO_4 and concentrated. The crude product was purified by neutral silica gel column chromatography using 15% ethyl acetate in hexane to obtain 180 mg of pure compound **Me-*o*-CB-35** as red solid. Yield: 43%. Mp: >200 °C. ^{1}H NMR (400 MHz, CD_2Cl_2, δ ppm): 6.55 (t, $J = 4.0$ Hz, 1H), 6.51 (d, $J = 4.0$, Hz, 2H), 4.42 (s, 4H, $-CH_2$), 4.39 (q, $J = 8.0$ Hz, 4H, $-CH_{2ester}$), 4.07 (s, 2H, C_{cage}–H), 1.98 (s, 6H, $-CH_{3pyrrole}$), 1.42 (s, 6H, $-CH_{3pyrrole}$), 1.37 (t, $J = 8.0$ Hz, 6H, $-CH_{3ester}$). ^{13}C NMR (100 MHz, CD_2Cl_2, δ ppm): 162.0, 159.4, 146.0, 145.8, 142.1, 137.1, 132.5, 129.4, 108.1, 103.2, 71.3 (C_{cage}–C), 69.6, 62.1, 58.6 (C_{cage}–C), 13.9, 12.2, 9.3. ^{11}B NMR (128 MHz, CD_2Cl_2, proton decoupled): −0.85 (t, $J = 28.2$ Hz, BF_2), −3.08, −4.30, −9.51, −10.69, −13.25(C_{cage}–B). ^{19}F NMR (376 MHz, CD_2Cl_2, δ ppm): −141.25 (q, $J = 26.3$ Hz). IR (KBr): 2987, 2925, 2848, 2593 (B–H), 1664, 1438, 1385, 1243, 1163, 1020, 773 cm^{-1}. HRMS (*m*/*z*): calcd for $C_{31}H_{51}B_{21}N_2F_2O_6$: 812.5820, found 812.5617 [M^+].

Data availability

The data supporting this article have been included as part of the ESI.†

Conflicts of interest

The authors report no conflict of interest.

Acknowledgements

Author RS would like to thank SERB-POWER, Science & Engineering Research Board, India (grant numbers: SPG/2021/002579), the Council of Scientific & Industrial Research, India (grant number: 02(0308)/17/EMR-II), the Higher Education Department, Government of Odisha, grant number: 26913/HED/HEPTC-WB-02-17 (OHEPEE), Science and Technology Department, Government of Odisha (grant no. ST-SCST-MISC. 0036-2023) and LSRB (grant number: LSRB-431/BTB/2024) for their financial support. The author BPD is thankful to Odisha State Higher Education Council for the extramural research funding under MRIP-2023 (grant number: 23EM/CH/16) for financial support. The author RS also acknowledges DST, FIST-New Delhi (SR/FST/CSI-243/2012) for providing NMR facility to Ravenshaw University, Cuttack.

References

1 J. Poater, M. Solà, C. Viñas and F. Teixidor, *Angew. Chem., Int. Ed.*, 2014, **53**, 12191–12195.
2 R. N. Grimes, in *Carboranes*, Elsevier, 2016, pp. 283–502.
3 B. Bhusan Jena and R. Satapathy, *ChemistrySelect*, 2023, **8**, e202302310.
4 B. B. Jena, S. R. Jena, B. R. Swain, C. S. Mahanta, L. Samanta, B. P. Dash and R. Satapathy, *Appl. Organomet. Chem.*, 2020, **34**, e5754.
5 B. P. Dash, R. Satapathy, B. P. Bode, C. T. Reidl, J. W. Sawicki, A. J. Mason, J. A. Maguire and N. S. Hosmane, *Organometallics*, 2012, **31**, 2931–2935.
6 B. R. Swain, C. S. Mahanta, B. B. Jena, S. K. Beriha, B. Nayak, R. Satapathy and B. P. Dash, *RSC Adv.*, 2020, **10**, 34764–34774.
7 M. F. Hawthorne, *Angew Chem. Int. Ed. Engl.*, 1993, **32**, 950–984.
8 P. Stockmann, M. Gozzi, R. Kuhnert, M. B. Sárosi and E. Hey-Hawkins, *Chem. Soc. Rev.*, 2019, **48**, 3497–3512.
9 A. Marfavi, P. Kavianpour and L. M. Rendina, *Nat. Rev. Chem*, 2022, **6**, 486–504.
10 F. Ali, N. S Hosmane and Y. Zhu, *Molecules*, 2020, **25**, 828.
11 N. S. Hosmane and R. Eagling, *Handbook of Boron Science: With Applications in Organometallics, Catalysis, Materials and MedicineVolume 1: Boron in Organometallic Chemistry*, World Scientific, Europe, 2018, vol. 1.
12 Y. Chen, F. Du, L. Tang, J. Xu, Y. Zhao, X. Wu, M. Li, J. Shen, Q. Wen, C. H. Cho and Z. Xiao, *Mol. Ther.–Oncolytics*, 2022, **24**, 400–416.
13 B. P. Dash, R. Satapathy, E. R. Gaillard, K. M. Norton, J. A. Maguire, N. Chug and N. S. Hosmane, *Inorg. Chem.*, 2011, **50**, 5485–5493.
14 B. P. Dash, R. Satapathy, E. R. Gaillard, J. A. Maguire and N. S. Hosmane, *J. Am. Chem. Soc.*, 2010, **132**, 6578–6587.
15 B. B. Jena, L. Satish, C. S. Mahanta, B. R. Swain, H. Sahoo, B. P. Dash and R. Satapathy, *Inorg. Chim. Acta*, 2019, **491**, 52–58.
16 P. Bauduin, S. Prevost, P. Farràs, F. Teixidor, O. Diat and T. Zemb, *Angew. Chem., Int. Ed.*, 2011, **50**, 5298–5300.
17 A. M. Cioran, A. D. Musteti, F. Teixidor, Ž. Krpetić, I. A. Prior, Q. He, C. J. Kiely, M. Brust and C. Viñas, *J. Am. Chem. Soc.*, 2012, **134**, 212–221.
18 J. J. Schwartz, A. M. Mendoza, N. Wattanatorn, Y. Zhao, V. T. Nguyen, A. M. Spokoyny, C. A. Mirkin, T. Baše and P. S. Weiss, *J. Am. Chem. Soc.*, 2016, **138**, 5957–5967.
19 C. J. Villagómez, T. Sasaki, J. M. Tour and L. Grill, *J. Am. Chem. Soc.*, 2010, **132**, 16848–16854.
20 E. A. Qian, A. I. Wixtrom, J. C. Axtell, A. Saebi, D. Jung, P. Rehak, Y. Han, E. H. Moully, D. Mosallaei, S. Chow, M. S. Messina, J. Y. Wang, A. T. Royappa, A. L. Rheingold, H. D. Maynard, P. Král and A. M. Spokoyny, *Nat. Chem.*, 2017, **9**, 333–340.
21 A. Saha, E. Oleshkevich, C. Vinas and F. Teixidor, *Adv. Mater.*, 2017, **29**, 1704238.
22 H. Jude, H. Disteldorf, S. Fischer, T. Wedge, A. M. Hawkridge, A. M. Arif, M. F. Hawthorne, D. C. Muddiman and P. J. Stang, *J. Am. Chem. Soc.*, 2005, **127**, 12131–12139.
23 M. Koshino, T. Tanaka, N. Solin, K. Suenaga, H. Isobe and E. Nakamura, *Science*, 2007, **316**, 853.
24 L. Liang, A. Rapakousiou, L. Salmon, J. Ruiz, D. Astruc, B. P. Dash, R. Satapathy, J. W. Sawicki and N. S. Hosmane, *Eur. J. Inorg. Chem.*, 2011, **2011**, 3043–3049.
25 L. Wu, M. Holzapfel, A. Schmiedel, F. Peng, M. Moos, P. Mentzel, J. Shi, T. Neubert, R. Bertermann, M. Finze, M. A. Fox, C. Lambert and L. Ji, *Nat. Commun.*, 2024, **15**, 3005.
26 A. V. Zaitsev, S. S. Kiselev, A. F. Smol'yakov, Y. V. Fedorov, E. G. Kononova, Y. A. Borisov and V. A. Ol'shevskaya, *Org. Biomol. Chem.*, 2023, **21**, 4084–4094.
27 C. Bellomo, D. Zanetti, F. Cardano, S. Sinha, M. Chaari, A. Fin, A. Maranzana, R. Núñez, M. Blangetti and C. Prandi, *Dyes Pigm.*, 2021, **194**, 109644.
28 E. Berksun, I. Nar, A. Atsay, İ. Özçeşmeci, A. Gelir and E. Hamuryudan, *Inorg. Chem. Front.*, 2018, **5**, 200–207.
29 C. Bellomo, M. Chaari, J. Cabrera-González, M. Blangetti, C. Lombardi, A. Deagostino, C. Viñas, N. Gaztelumendi, C. Nogués, R. Nuñez and C. Prandi, *Chem.–Eur. J.*, 2018, **24**, 15622–15630.
30 Z. Xie, *Coord. Chem. Rev.*, 2002, **231**, 23–46.
31 Z. Xie, *Acc. Chem. Res.*, 2003, **36**, 1–9.
32 Z.-J. Yao and G.-X. Jin, *Coord. Chem. Rev.*, 2013, **257**, 2522–2535.
33 Z. Qiu, S. Ren and Z. Xie, *Acc. Chem. Res.*, 2011, **44**, 299–309.
34 J. Estrada and V. Lavallo, *Angew. Chem., Int. Ed.*, 2017, **56**, 9906–9909.
35 J. C. Axtell, K. O. Kirlikovali, P. I. Djurovich, D. Jung, V. T. Nguyen, B. Munekiyo, A. T. Royappa, A. L. Rheingold and A. M. Spokoyny, *J. Am. Chem. Soc.*, 2016, **138**, 15758–15765.
36 Y.-P. Zhou, S. Raoufmoghaddam, T. Szilvási and M. Driess, *Angew. Chem., Int. Ed.*, 2016, **55**, 12868–12872.
37 S. Kimura, S. Masunaga, T. Harada, Y. Kawamura, S. Ueda, K. Okuda and H. Nagasawa, *Bioorg. Med. Chem.*, 2011, **19**, 1721–1728.
38 Y. Hattori, S. Kusaka, M. Mukumoto, K. Uehara, T. Asano, M. Suzuki, S. Masunaga, K. Ono, S. Tanimori and M. Kirihata, *J. Med. Chem.*, 2012, **55**, 6980–6984.
39 T. He and R. A. Musah, *ACS Omega*, 2019, **4**, 3820–3826.
40 S. M. Hillier, K. P. Maresca, F. J. Femia, J. C. Marquis, C. A. Foss, N. Nguyen, C. N. Zimmerman, J. A. Barrett, W. C. Eckelman, M. G. Pomper, J. L. Joyal and J. W. Babich, *Cancer Res.*, 2009, **69**, 6932–6940.
41 T. Maurer, M. Eiber, M. Schwaiger and J. E. Gschwend, *Nat. Rev. Urol.*, 2016, **13**, 226–235.
42 M. Eder, M. Schäfer, U. Bauder-Wüst, W.-E. Hull, C. Wängler, W. Mier, U. Haberkorn and M. Eisenhut, *Bioconjugate Chem.*, 2012, **23**, 688–697.
43 S. Wang, C. Blaha, R. Santos, T. Huynh, T. R. Hayes, D. R. Beckford-Vera, J. E. Blecha, A. S. Hong, M. Fogarty, T. A. Hope, D. R. Raleigh, D. M. Wilson, M. J. Evans,

H. F. VanBrocklin, T. Ozawa and R. R. Flavell, *Mol. Pharmaceutics*, 2019, **16**, 3831–3841.
44 G. H. Vicente and M. Sibrian-Vazquez, in *Handbook of Porphyrin Science (Volume 4) with Applications to Chemistry, Physics, Materials Science, Engineering, Biology and Medicine*, World Scientific, 2010.
45 N. V. S. D. K. Bhupathiraju and M. G. H. Vicente, in *Applications of Porphyrinoids*, ed. R. Paolesse, Springer Berlin Heidelberg, Berlin, Heidelberg, 2013, vol. 34, pp. 31–52.
46 N. V. S. D. K. Bhupathiraju and M. G. H. Vicente, *Bioorg. Med. Chem.*, 2013, **21**, 485–495.
47 D.-Q. Wu, B. Lu, C. Chang, C.-S. Chen, T. Wang, Y.-Y. Zhang, S.-X. Cheng, X.-J. Jiang, X.-Z. Zhang and R.-X. Zhuo, *Biomaterials*, 2009, **30**, 1363–1371.
48 A. A. D'Souza and P. V. Devarajan, *J. Controlled Release*, 2015, **203**, 126–139.
49 T. Zhang, G. Li, S. Li, Z. Wang, D. He, Y. Wang, J. Zhang, J. Li, Z. Bai, Q. Zhang, B. Liu, Q. Zhao, Y. Liu and H. Zhang, *Colloids Surf., B*, 2019, **182**, 110397.
50 V. V. Mody, A. Cox, S. Shah, A. Singh, W. Bevins and H. Parihar, *Appl. Nanosci.*, 2014, **4**, 385–392.
51 X. Chen, X. Bao, J.-C. Zhao and S. G. Shore, Experimental and Computational Study of the Formation Mechanism of the Diammoniate of Diborane, **https://pubs.acs.org/doi/pdf/10.1021/ja203648w**, accessed July 28, 2024.
52 H. Kuang, S. Wu, Z. Xie, F. Meng, X. Jing and Y. Huang, *Biomacromolecules*, 2012, **13**, 3004–3012.
53 H. Xiong, D. Zhou, Y. Qi, Z. Zhang, Z. Xie, X. Chen, X. Jing, F. Meng and Y. Huang, *Biomacromolecules*, 2015, **16**, 3980–3988.
54 I. Nakase, M. Katayama, Y. Hattori, M. Ishimura, S. Inaura, D. Fujiwara, T. Takatani-Nakase, I. Fujii, S. Futaki and M. Kirihata, *Chem. Commun.*, 2019, **55**, 13955–13958.
55 H. Koganei, M. Ueno, S. Tachikawa, L. Tasaki, H. S. Ban, M. Suzuki, K. Shiraishi, K. Kawano, M. Yokoyama, Y. Maitani, K. Ono and H. Nakamura, *Bioconjugate Chem.*, 2013, **24**, 124–132.
56 B. R. Swain, S. R. Jena, S. K. Beriha, C. S. Mahanta, B. B. Jena, T. Prasanth, L. Samanta, R. Satapathy and B. P. Dash, *New J. Chem.*, 2023, **47**, 10296–10308.
57 R. Dubey, S. Kushal, A. Mollard, L. Vojtovich, P. Oh, M. D. Levin, J. E. Schnitzer, I. Zharov and B. Z. Olenyuk, *Bioconjugate Chem.*, 2015, **26**(1), 78–89.
58 R. Satapathy, B. P. Dash, C. S. Mahanta, B. R. Swain, B. B. Jena and N. S. Hosmane, *J. Organomet. Chem.*, 2015, **798**, 13–23.
59 A. R. Genady and M. E. El-Zaria, *Appl. Organomet. Chem.*, 2008, **22**, 227–232.
60 S. Stadlbauer, P. Welzel and E. Hey-Hawkins, *Inorg. Chem.*, 2009, **48**, 5005–5010.
61 J. H. Gibbs, H. Wang, N. V. S. D. K. Bhupathiraju, F. R. Fronczek, K. M. Smith and M. G. H. Vicente, *J. Organomet. Chem.*, 2015, **798**, 209–213.
62 S. Xuan, N. Zhao, Z. Zhou, F. R. Fronczek and M. G. H. Vicente, *J. Med. Chem.*, 2016, **59**, 2109–2117.
63 M. Shirakawa, A. Zaboronok, K. Nakai, Y. Sato, S. Kayaki, T. Sakai, T. Tsurubuchi, F. Yoshida, T. Nishiyama, M. Suzuki, H. Tomida and A. Matsumura, *Cells*, 2021, **10**, 3421.
64 M. Couto, M. F. García, C. Alamón, M. Cabrera, P. Cabral, A. Merlino, F. Teixidor, H. Cerecetto and C. Viñas, *Chem.–Eur. J.*, 2018, **24**, 3122–3126.
65 M. Couto, I. Mastandrea, M. Cabrera, P. Cabral, F. Teixidor, H. Cerecetto and C. Viñas, *Chem.–Eur. J.*, 2017, **23**, 9233–9238.
66 C. S. Mahanta, S. Aparna, S. K. Das, B. B. Jena, B. R. Swain, M. Patri, B. P. Dash and R. Satapathy, *ChemistrySelect*, 2020, **5**, 8429–8434.
67 E. Antina, N. Bumagina, Y. Marfin, G. Guseva, L. Nikitina, D. Sbytov and F. Telegin, *Molecules*, 2022, **27**, 1396.
68 V. I. Martynov and A. A. Pakhomov, *Russ. Chem. Rev.*, 2021, **90**, 1213–1262.
69 D. Dai, G. Lian, X. He, J. Feng and G. Jin, *Photochem. Photobiol. Sci.*, 2022, **21**, 185–194.
70 T. Kowada, H. Maeda and K. Kikuchi, *Chem. Soc. Rev.*, 2015, **44**, 4953–4972.
71 P. Kaur and K. Singh, *J. Mater. Chem. C*, 2019, **7**, 11361–11405.
72 S. Kolemen and E. U. Akkaya, *Coord. Chem. Rev.*, 2018, **354**, 121–134.
73 A. N. Kursunlu, Z. E. Koc, A. Y. Obalı and E. Güler, *J. Lumin.*, 2014, **149**, 215–220.
74 J. L. Donnelly, D. Offenbartl-Stiegert, J. M. Marín-Beloqui, L. Rizzello, G. Battaglia, T. M. Clarke, S. Howorka and J. D. Wilden, *Chem.–Eur. J.*, 2020, **26**, 863–872.
75 E. R. Thapaliya, Y. Zhang, P. Dhakal, A. S. Brown, J. N. Wilson, K. M. Collins and F. M. Raymo, *Bioconjugate Chem.*, 2017, **28**, 1519–1528.
76 Y. Ni and J. Wu, *Org. Biomol. Chem.*, 2014, **12**, 3774.
77 J. Zhang, L. Wang and Z. Xie, *ACS Biomater. Sci. Eng.*, 2018, **4**, 1969–1975.
78 V. Nguyen, Y. Yim, S. Kim, B. Ryu, K. M. K. Swamy, G. Kim, N. Kwon, C. Kim, S. Park and J. Yoon, *Angew. Chem., Int. Ed.*, 2020, **59**, 8957–8962.
79 Y. Liu, N. Song, L. Chen, S. Liu and Z. Xie, *Chem.–Asian J.*, 2018, **13**, 989–995.
80 M. A. Masood, Y. Wu, Y. Chen, H. Yuan, N. Sher, F. Faiz, S. Yao, F. Qi, M. I. Khan, M. Ahmed, N. Mushtaq, W. He and Z. Guo, *Dyes Pigm.*, 2022, **202**, 110255.
81 Y. Qin, X. Liu, P.-P. Jia, L. Xu and H.-B. Yang, *Chem. Soc. Rev.*, 2020, **49**, 5678–5703.
82 R. Prieto-Montero, A. Prieto-Castañeda, R. Sola-Llano, A. R. Agarrabeitia, D. García-Fresnadillo, I. López-Arbeloa, A. Villanueva, M. J. Ortiz, S. De La Moya and V. Martínez-Martínez, *Photochem. Photobiol.*, 2020, **96**, 458–477.
83 L. Collado, T. Naranjo, M. Gomez-Mendoza, C. G. López-Calixto, F. E. Oropeza, M. Liras, J. Marugán and V. A. De La Peña O'Shea, *Adv. Funct. Mater.*, 2021, **31**, 2105384.
84 K. Ladomenou, V. Nikolaou, G. Charalambidis, A. Charisiadis and A. G. Coutsolelos, *C. R. Chim.*, 2017, **20**, 314–322.

85 J.-Y. Liu, X.-N. Hou, Y. Tian, L. Jiang, S. Deng, B. Röder and E. A. Ermilov, *RSC Adv.*, 2016, **6**, 57293–57305.
86 G. Kalot, A. Godard, B. Busser, J. Pliquett, M. Broekgaarden, V. Motto-Ros, K. D. Wegner, U. Resch-Genger, U. Köster, F. Denat, J.-L. Coll, E. Bodio, C. Goze and L. Sancey, *Cells*, 2020, **9**, 1953.
87 M. Prieto-Vila, R. Takahashi, W. Usuba, I. Kohama and T. Ochiya, *Int. J. Mater. Sci.*, 2017, **18**, 2574.
88 J. L. Griffin and J. P. Shockcor, *Nat. Rev. Cancer*, 2004, **4**, 551–561.
89 J. S. You and P. A. Jones, *Cancer Cell*, 2012, **22**, 9–20.
90 G. H. Williams and K. Stoeber, *J. Pathol.*, 2012, **226**, 352–364.
91 T. Otto and P. Sicinski, *Nat. Rev. Cancer*, 2017, **17**, 93–115.
92 U. Raju, E. Nakata, K. A. Mason, K. K. Ang and L. Milas, *Cancer Res.*, 2003, **63**, 3263–3267.
93 C. Dittrich, M. Gneist, A. Zandvliet, C. Johnston and M. Yule, *Eur. J. Cancer Suppl.*, 2004, **2**, 129.
94 M. A. Dickson and G. K. Schwartz, *Curr. Oncol.*, 2009, **16**, 36–43.
95 Q. Chen, T. Wang, Y. Zhang, Q. Wang and J. Ma, *Synth. Commun.*, 2002, **32**, 1031–1040.
96 A. G. Joseph, M. Biji, V. P. Murali, D. R. Sherin, A. Valsan, V. P. Sukumaran, K. V. Radhakrishnan and K. K. Maiti, *RSC Med. Chem.*, 2024, **15**, 3444–3459.
97 A. E. Mercier, A. M. Joubert, R. Prudent, J. Viallet, A. Desroches-Castan, L. De Koning, P. Mabeta, J. Helena, M. S. Pepper and L. Lafanechère, *Cancers*, 2024, **16**, 2941.
98 T. Gebäck, M. M. P. Schulz, P. Koumoutsakos and M. Detmar, *BioTechniques*, 2009, **46**, 265–274.
99 C. Bertoli, J. M. Skotheim and R. A. M. De Bruin, *Nat. Rev. Mol. Cell Biol.*, 2013, **14**, 518–528.
100 H. Wang, M. Guo, H. Wei and Y. Chen, *Signal Transduction Targeted Ther.*, 2023, **8**, 92.
101 T. Ozaki and A. Nakagawara, *Cancers*, 2011, **3**, 994–1013.
102 F. Hoppe-Seyler and K. Butz, *J. Virol.*, 1993, **67**, 3111–3117.
103 A. K. Ajay, A. S. Meena and M. K. Bhat, *Cell Biosci.*, 2012, **2**, 2.
104 S. A. Mujib, F. Alamsyah and W. P. Taruno, *Integr. Med. Int.*, 2017, **4**, 161–170.
105 A. V. Zaitsev, E. G. Kononova, A. A. Markova, A. V. Shibaeva, A. A. Kostyukov, A. E. Egorov, V. A. Kuzmin, A. A. Shtil and V. A. Ol'shevskaya, *Dyes Pigm.*, 2022, **207**, 110711.
106 G. Barrera, *ISRN Oncol.*, 2012, **2012**, 1–21.